The Astrophysical Journal Letters, 1002:L34 (21pp), 2026 May 10 https://doi.org/10.3847/2041-8213/ae5dcc
© 2026. The Author(s). Published by the American Astronomical Society.
OPEN ACCESS

# A Systematic Search for Trace Molecules in the Atmosphere of Exoplanet K2-18 b

Lorenzo Pica-Ciamarra, Nikku Madhusudhan, Gregory J. Cooke, Savvas Constantinou, and Martin Binet
Institute of Astronomy, University of Cambridge, Madingley Road, Cambridge CB3 0HA, UK; nmadhu@ast.cam.ac.uk
*Received 2025 May 15; revised 2026 March 18; accepted 2026 April 4; published 2026 May 8*

## Abstract

The first transmission spectrum of the habitable-zone sub-Neptune K2-18 b with JWST has opened a new avenue for atmospheric characterisation of temperate low-mass exoplanets. The observations led to inferences of methane and carbon dioxide, as well as of dimethyl sulfide (DMS) and/or dimethyl disulfide, both potential biosignatures. In the present work we conduct a broad and agnostic search for other chemical species in the atmosphere of K2-18 b. Our exploration includes 661 molecules, spanning a wide range of trace gases, including biotic, abiotic, and anthropogenic gases on Earth. We investigate possible preference for any of these gases, compared to a model only including the previously detected $CH_4$ and $CO_2$, using three metrics: (a) preference in the JWST mid-infrared (MIR) spectrum, (b) preference in the JWST near-infrared (NIR) spectrum, for species preferred in MIR, and (c) plausible sources of production. We find that only DMS consistently results in Bayes factors $\ln B \geqslant 2.0$ across the datasets considered independently, though in the NIR this depends on detector offsets, as previously reported. The threshold of $\ln B \geqslant 2.0$ is motivated by the conventional threshold of $\ln B \geqslant 2.5$ for moderate preference, allowing for an empirical uncertainty of 0.5. A few other gases also provide comparable fits to a subset of the data or only with some of the retrieval codes used, but with limited known plausible sources. Our study highlights the need for further observations to distinguish between possible trace gases in the atmosphere of K2-18 b as well as theoretical work to establish their plausible sources.

*Unified Astronomy Thesaurus concepts:* Exoplanets (498); Habitable planets (695); Exoplanet atmospheres (487); Exoplanet atmospheric composition (2021)

## 1. Introduction

The atmospheric characterization of temperate ($T_{\rm eq} \lesssim 400$ K) planets is the new frontier of exoplanet science. Sub-Neptune planets are the largest class of currently known exoplanets (e.g., B. J. Fulton & E. A. Petigura 2018), but they have no analog in the solar system, such that any empirical insights into their nature must come from remote atmospheric observations. The start of JWST operations has led to a revolution in our ability to characterize temperate sub-Neptune atmospheres. JWST near-infrared (NIR) observations of the habitable-zone planet K2-18 b have led to the first detections of carbon-bearing molecules ($CO_2$ and $CH_4$) in a temperate sub-Neptune (N. Madhusudhan et al. 2023, hereafter M23), with tentative evidence for dimethyl sulfide (DMS), a possible biosignature gas (C. B. Pilcher 2003; S. D. Domagal-Goldman et al. 2011; S. Seager et al. 2013). S. P. Schmidt et al. (2025) disputed this finding, claiming no evidence for $CO_2$ and DMS. However, a later analysis by R. Hu et al. (2025), which considered additional NIR observations, confirmed the initial results presented in M23. Similar results to K2-18 b were obtained for the temperate sub-Neptune TOI-270 d, with the analysis of JWST NIR spectra revealing $CH_4$ and $CO_2$, as well as tentative inferences of $CS_2$ and $H_2O$ (M. Holmberg & N. Madhusudhan 2024; B. Benneke et al. 2024).

More recently, the first observations have been reported in the mid-infrared (MIR) for a temperate sub-Neptune, (N. Madhusudhan et al. 2025, hereafter M25) with the JWST MIRI spectrum of K2-18 b. They reported evidence for the presence of DMS and/or dimethyl disulfide (DMDS), both possible biosignature gases (C. B. Pilcher 2003; S. D. Domagal-Goldman et al. 2011), at a $3\sigma$ significance compared to a model including $CH_4$ and $CO_2$ only. However, each of these two molecules individually is only tentatively inferred due to the degeneracy between their spectral features (M25), requiring further observations for a more robust assessment. In particular, R. Luque et al. (2025), performing a joint analysis of the data, found that the results are dominated by the NIR spectrum, and the evidence for presence of DMS depends on the adopted data reduction pipeline, ranging between no evidence and moderate ($\ln B = 2.8$) evidence, consistent with or higher than the corresponding retrieval in M23 with the NIR data alone. New observations in the NIR presented in R. Hu et al. (2025) can also provide, depending on the model used, up to $\ln B = 3.5$ preference for a combination of DMS, $N_2O$, and $CH_3SH$ over a model only including six standard CNO species ($CH_4$, $CO_2$, CO, $NH_3$, HCN, and $H_2O$). These observations open a new avenue for studying habitable-zone exoplanets, including the search for biosignatures in their atmospheres.

The MIRI observations of K2-18 b are at the frontier of the capabilities of JWST and test the limits of its sensitivity. As such, they represent the most advanced analysis possible for habitable-zone exoplanets with present facilities. However, given their low signal-to-noise ratio and low resolution, these datasets also open new challenges. For example, as evidenced by the low significance of the DMS and DMDS inferences (M25; R. Hu et al. 2025; R. Luque et al. 2025), follow-up efforts are needed both to increase the quality of the observations as well as to robustly interpret them. Efforts in this direction (J. Taylor 2025, hereafter T25; L. Welbanks et al. 2026, hereafter W26) have explored agnostic approaches to find alternative interpretations for the existing data. While both the T25 and the W26 approaches are agnostic, they rely on different levels of model complexity and physical plausibility. On the one hand, T25 consider parametric

Original content from this work may be used under the terms of the Creative Commons Attribution 4.0 licence. Any further distribution of this work must maintain attribution to the author(s) and the title of the work, journal citation and DOI.

Gaussian models to fit the MIRI transmission spectrum, finding up to $\sim 2\sigma$ Bayesian preference for a model with features compared to a flat line. While the negative Gaussian models reported in T25 are unphysical, the study nevertheless serves the purpose of independently verifying the potential for spectral features in the data.

On the other hand, W26 pursue a different approach by exploring a larger suite of molecules than the 20 explored in M25. At the outset, W26 reproduce an $\sim 3\sigma$ preference for models including DMS and/or DMDS in addition to $CO_2$ and $CH_4$, relative to a baseline model with only $CH_4$ and $CO_2$ included, as reported in M25. In addition, W26 also find three other molecules with $\ln B \geqslant 2.5$ preference (equivalent to $2.8\sigma$ significance, when using the inverse T. Sellke et al. 2001 and R. Trotta 2008 conversion), corresponding to the lower threshold for moderate evidence (R. Trotta 2008), over the baseline model. For these cases, they find significances between $2.8\sigma$ and $3.1\sigma$, which are comparable to their equivalent significances of $2.7\sigma$–$3.0\sigma$ for DMS, DMDS, or DMS + DMDS, considering a typical error of $0.1\sigma$–$0.2\sigma$ in such calculations (M25). The exploration of W26 focused only on the MIRI data reported in M25. Therefore, open questions remain on the robustness of their findings when the NIR data reported in M23 are considered.

As discussed in M25, such agnostic explorations are important to establish the space of possible explanations to the data. However, the physical plausibility of most of the 90 hydrocarbons considered in W26 for an exoplanetary atmosphere remains unclear. For example, among the three gases they find above the threshold for moderate model preference, only propyne was discussed as potentially plausible in the atmosphere of K2-18 b. The remaining gases are produced in small quantities on Earth, primarily biotic or anthropogenic, with few sources known in other planetary environments. We discuss the physical plausibility of these gases in Section 5.3. Furthermore, while W26 focused on hydrocarbons, the much larger space of molecules involving other prominent elements, including N and S, remains unexplored.

A reliable inference of a chemical signature in an exoplanetary atmosphere requires consideration of all the available data and an assessment of its feasibility in the given context. In the present work, we report a systematic and wide-ranging search for trace molecules in the atmosphere of K2-18 b using all available transmission spectra with JWST reported in M23 and M25. We conduct in-depth and agnostic atmospheric retrievals exploring a large ensemble of 661 molecules, spanning molecules with abiotic, biotic, and anthropogenic sources on Earth. We assess the molecules based on multiple lines of evidence, across the available datasets and multiple retrieval frameworks, and their physical plausibility in the context of K2-18 b.

In what follows, we begin, in Section 2, with a discussion of prevalent practices with regards to model selection, standards of evidence, and biosignature assessment, in the characterization of exoplanetary atmospheres. Next, in Section 3, we describe the protocol for our systematic search and the retrieval approach. We present our results in Section 4 and discuss their physical plausibility in Section 5. We summarize our work and discuss future directions in Section 6.

## 2. Considerations from Previous Work

The launch of JWST (J. P. Gardner et al. 2006) has opened a new era in the characterization of exoplanetary atmospheres. The quality of available data requires new efforts in establishing appropriate methods for their analysis. The spectroscopic capability of JWST instruments spans a wide range, from higher-resolution NIRISS ($R \sim 700$ for NIRISS SOSS) and NIRSpec ($R \sim 2700$ with high-resolution gratings) spectroscopy in the NIR to low-resolution spectroscopy and photometry with MIRI ($R \sim 100$ for MIRI Low Resolution Spectroscopy (LRS)) in the MIR. The presently available MIRI LRS spectra, in particular, can sometimes be comparable in data quality to the best Hubble Space Telescope (HST) spectra of exoplanets obtained in the pre-JWST era, with significantly lower observing time and much broader wavelength range. It is thus pertinent to review prevalent practices on the analysis and interpretation of such data in order to inform the next steps toward the characterization of exoplanetary atmospheres with JWST.

### 2.1. Model Selection

A central consideration in atmospheric retrievals of exoplanets is the complexity and dimensionality of the model considered given the data at hand. Atmospheric retrievals of low-mass exoplanets in the pre-JWST era provided initial insights into the model requirements. In the case of the sub-Neptune K2-18 b, early retrievals were conducted using a low-resolution spectrum obtained with HST WFC3 (B. Benneke et al. 2019; A. Tsiaras et al. 2019; N. Madhusudhan et al. 2020). The nominal model in B. Benneke et al. (2019) included as free parameters the mixing ratios for seven chemical species, the cloud-top pressure for a gray cloud deck, and an isothermal $P$–$T$ profile, for a total of nine free parameters. On the other hand, the largest model in A. Tsiaras et al. (2019) considered free mixing ratios for five species, and their nominal model included only two species. As another example, N. Madhusudhan et al. (2020) included free mixing ratios for five species, as well as a nonisothermal $P$–$T$ profile and inhomogeneous clouds, for a total of 16 free parameters.

With the advent of JWST, unprecedented data quality was obtained in the NIR, which led to significantly more complex models for atmospheric retrievals. For example, M23 considered the mixing ratios of 11 species as free parameters when performing atmospheric retrievals on the atmosphere of K2-18 b. However, the presently available data obtained from the MIR instrument, MIRI LRS, is of comparable quality to the NIR HST WFC3 data, albeit at a fraction of the observing time. As model complexity (e.g., the number of free parameters included in the model) needs to match data quality (e.g., the spectral resolution and signal-to-noise ratio of available data), retrieval setups used for the analysis of comparable HST WFC3 data act as a good guideline for the appropriate choices when analyzing JWST MIRI LRS data. This has indeed been followed in the atmospheric characterization of hot Jupiter WASP-17 b with a dataset including both JWST MIRI and HST WFC3 data, which used models including 4–7 molecules (D. Grant et al. 2023). An even simpler setup was adopted in several of the models considered by D. Powell et al. (2024), which only included two species, $H_2O$ and $SO_2$.

In the abovementioned cases, the selection of species to be included in the atmospheric retrievals was broadly based on thermochemical and/or photochemical expectations for the planets being studied. The analysis of MIRI LRS data of K2-18 b by M25, working with data of similar quality to those analyzed in the studies mentioned above, attempted to formalize the model selection process. In order to do so, M25 introduced a new approach, which is also more conducive to the exploration of a larger parameter space.

M25 started by considering a "maximal" model, which included 20 species, the largest set at the time for JWST observations of sub-Neptunes. Inspection of the posterior distributions revealed that only one species, DMDS, showed a clear peak. In order to identify other potential contributors to the spectrum, DMDS was removed from the model. This led to DMS showing a peak in the posterior distribution, upon the removal of which no other molecules stood out. A simpler model with four species, including $CH_4$ and $CO_2$, inferred in the NIR by M23, and DMS and DMDS, was then considered. This canonical model was found to be preferred at a $2\sigma$ level over the maximal model. Following Occam's razor, this simpler case was adopted as the canonical model, against which to compute model preferences; for a discussion on model complexity in a Bayesian setting, see R. Trotta (2008). This canonical model is of similar complexity, and includes a similar number of molecules, to what was used in N. Madhusudhan et al. (2020) and D. Grant et al. (2023), for comparable data quality. In addition, M25 also noted the strong degeneracy between DMS and DMDS in the MIRI band and, therefore, explored canonical models with only one of DMS or DMDS included besides $CH_4$ and $CO_2$.

Later, W26 investigated the M25 observations through a new maximal model, with 21 species and 33 free parameters, and also through an array of 93 canonical models. These models were similar to the M25 canonical model, in that each included three chemical species: $CH_4$, $CO_2$, and each of 92 species, one by one, to assess whether the MIRI data provided any evidence for their presence. The 92 species included DMS and DMDS, and W26 also considered a case where both DMS and DMDS were included, corresponding to a similar case used by M25. They successfully replicated the M25 findings that DMS, DMDS, and their combination are preferred at $\sim 3\sigma$ over a model only including $CH_4$ and $CO_2$. We note that this is to be expected, given that the `Aurora` retrieval framework used in W26 belongs to the same family as the `AURA` retrieval code used in M25. In addition, however, they found three other molecules, not previously explored by M25, for which the data provided at least moderate evidence ($\geqslant 2.7\sigma$ according to Jeffreys' scale; see, e.g., R. Trotta 2008).

Overall, the model complexity in atmospheric retrievals needs to be motivated by the data quality. As shown in M25, while a maximal model with 20 species is useful for the exploration of a wide parameter space, it may be less favored in a Bayesian sense than a model whose complexity better matches the data quality, e.g., a nested model including only the few most relevant molecules. Furthermore, for a large exploration of chemical species, e.g., hundreds of species, a retrieval including all the molecules at once is computationally infeasible currently. Choices of maximal models are thus necessarily arbitrary. For example, while M25 included 20 relevant species, future studies could include other plausible molecules, such as isoprene (Z. Zhan et al. 2021), propyne (Z. Huang et al. 2024), or benzene (S.-M. Tsai et al. 2024). Therefore, the approach of selecting a minimal canonical model informed by theoretical and empirical considerations serves a good starting point at the present time, although it is important to ensure that these are not exceedingly simple (e.g., L. Welbanks & N. Madhusudhan 2019, 2022). Such minimal models, in turn, can be used for exploring a wide array of species sequentially, thus identifying promising candidate species for further investigation, as pursued in M25 and W26.

### 2.2. Detection Significances

The question of what degree of statistical significance is to be considered enough to claim a discovery is a question every scientific discipline has had to address. The standards vary widely across fields: in biological and medical research, for example, a result with a $p$-value of $p < 0.05$, corresponding to a $2\sigma$ result, is often considered acceptable, despite doubts as to the appropriateness of this threshold (R. A. Fisher 1934; V. Amrhein et al. 2017). On the other hand, in experimental high-energy physics, significances of $\geqslant 5\sigma$ are required to claim a discovery (Particle Data Group et al. 2022).

Until recently, the consensus in the field of exoplanet atmospheres seemed to be that the threshold for a chemical detection lied somewhere between $\sim 2\sigma$ and $3\sigma$, as determined by converting the relevant Bayesian model preference (see, e.g., R. Trotta 2008; B. Benneke & S. Seager 2013). For example, D. Grant et al. (2023) claimed a detection of quartz clouds in the atmosphere of hot Jupiter WASP-17 b through a JWST MIRI spectrum, when the model with quartz clouds was preferred at $2.6\sigma$ over a (nonnested) model only including a generic aerosol parameterization. Similarly, D. Powell et al. (2024) considered $SO_2$ to have been detected in the MIRI spectrum of WASP-39 b with significance values varying between $2.5\sigma$ and $4.21\sigma$, depending on the choice of retrieval code and data reduction pipeline. More recently, R. Liu et al. (2025) referred to both a $3.09\sigma$ preference for $H_2O$ and a $1.90\sigma$ preference for a gray cloud deck in the hot Jupiter HAT-P-14 b as detections. Similarly, M. M. Murphy et al. (2025) reported a detection of $H_2O$ in the atmosphere of hot Neptune HD 219666 b, based on a model preference of $2.9\sigma$. In all these cases, as discussed above, the number of molecules considered in the models ranged between four and seven. We highlight that, in all cases discussed, detection significances were obtained by Bayesian model comparison, which provides a metric for the preference of a model compared to a reference model.

The recent inferences of chemical signatures in the sub-Neptune K2-18 b (M23, M25) have motivated a reconsideration of what statistical significance constitutes a reliable detection. For example, S. P. Schmidt et al. (2025) advocate for adopting a higher significance to claim detections of chemical species in exoplanet atmospheres. This represents a shift from the standard employed in earlier works using similar retrieval frameworks, such as D. Grant et al. (2023) and M. M. Murphy et al. (2025). A reasonable approach would be to follow the conventional metric of Jeffreys' scale in Bayesian inference of considering a significance between $2.7\sigma$ and $3.6\sigma$ as moderate evidence, and at and above $3.6\sigma$ as strong evidence (e.g., R. Trotta 2008). However, Bayesian model selection itself is not free from pitfalls, and caution needs to be exercised when applying it (e.g., G. Efstathiou 2008; L. Welbanks et al. 2023; A. Dittmann 2024; M. C. Nixon et al. 2024; D. P. Thorngren et al. 2026). For any

approach chosen, it is also important to use the same metric across all chemical inferences to ensure a uniform standard in the field.

### 2.3. Biosignatures in Context

A central question in the field is about what molecules at what abundances can be regarded as robust biosignatures, i.e., unambiguous indicators of the presence of life. Various studies in the past have suggested criteria to conclusively identify a biosignature (e.g., S. Seager et al. 2016; D. C. Catling et al. 2018; V. Meadows et al. 2022). Most recently, S. Seager et al. (2025) reiterated three criteria that need to be met for a detected molecule to be considered as a robust biosignature: (a) it has a distinctive spectral feature versus the dominant gas, (b) it has a plausible production rate, and (c) it has no known significant false positives in the given planetary context.

A number of molecules produced primarily by life on Earth have been suggested in the past as reliable biosignatures for habitable exoplanets. These include molecules such as $N_2O$, DMS, and $CH_3Cl$ (e.g., S. D. Domagal-Goldman et al. 2011; S. Seager et al. 2013; D. C. Catling et al. 2018; M. Leung et al. 2022). The identification of a biosignature would be dependent on the specific context and environment, and rely on multiple lines of evidence (V. Meadows et al. 2022). However, what qualifies as a relevant abiotic source for a potential biosignature molecule remains an open question. Previous assessments of abiotic false positives included possible sources from geological or atmospheric processes, e.g., through photochemistry. For example, while $CH_4$ is predominantly produced by life on Earth, it is also produced in small quantities by geochemical sources and can be produced through atmospheric chemistry in $H_2$-rich environments (E. W. Schwieterman & M. Leung 2024). On the other hand, it is also important to ascertain that any proposed abiotic mechanism for an observed molecule is also physically plausible in the context of a given planetary atmosphere, and is consistent with the observed constraints.

The discussion around the molecule DMS in the habitable-zone sub-Neptune K2-18 b is a case in point. For two decades, DMS has been regarded as a robust biosignature across different environments, in both Earth-like and $H_2$-rich atmospheres (C. B. Pilcher 2003; S. D. Domagal-Goldman et al. 2011; S. Seager et al. 2016; D. C. Catling et al. 2018; N. Madhusudhan et al. 2021). However, the first inference of DMS in the atmosphere of K2-18 b (M23, M25) has prompted a reconsideration of its candidacy as a robust biosignature (S. Seager et al. 2025). Recently, S. Seager et al. (2025) argued that DMS is no longer a robust biosignature due to potential abiotic formation scenarios (see their Tables 1 and S2). S. Seager et al. (2025) supported this statement by highlighting the abiotic synthesis of DMS in laboratory photochemical experiments (F. Raulin & G. Toupance 1975; N. W. Reed et al. 2024), and its identification in a comet (N. Hänni et al. 2024) and the interstellar medium (ISM; M. Sanz-Novo et al. 2025). However, as discussed in M25 (their Section 4.2), neither the laboratory experiments nor the comet detection are able to explain the high inferred abundance of DMS (10–1000 ppm) in the context of the observed atmosphere of K2-18 b. Generally, the presence of a molecule on a comet or in the ISM does not by itself constitute a reliable false positive, given their vastly different environments compared to a dense planetary atmosphere, and the implausibility of volatile delivery and stability through cometary impacts (M. Leung et al. 2022; M25). A large number of complex organic compounds, including amino acids (A. Belloche et al. 2013; M. Guélin & J. Cernicharo 2022), which can be produced and remain stable in the cold and low-density environments of the ISM and comets (L. Le Roy et al. 2015) would be unlikely to remain stable and abundant in a planetary atmosphere. Finally, the closest experiment to the currently evaluated context produced DMS mixing ratios of 0.05 ppmv (N. W. Reed et al. 2024), at least 200 times lower than (or 0.5% of) the inferred DMS abundance and requiring the presence of $H_2S$, which has not been detected.

Furthermore, any criterion for the identification of a biosignature or a false positive needs to be applied consistently. For example, S. Seager et al. (2025) identify the following molecules as having no known significant false positives in a terrestrial context: $CH_3OH$, $PH_3$, $NH_3$, and potentially $CH_3Cl$, $CH_3Br$, and $N_2O$. However, other studies have shown that $NH_3$, $CH_3OH$, and $CH_3Cl$ are also present in comets (L. Le Roy et al. 2015; E. C. Fayolle et al. 2017), including the same comet where DMS was reported (N. Hänni et al. 2024, 2025), and $PH_3$ is present in the atmospheres of Jupiter and Saturn (S. S. Barshay & J. S. Lewis 1978; R. Courtin et al. 1984; G. S. Orton et al. 2000; F. Taylor et al. 2004). It may be reasonable to suggest $NH_3$ (e.g., J. Huang et al. 2022) or $PH_3$ (e.g., C. Sousa-Silva et al. 2020) as biosignatures for terrestrial exoplanets, like Earth and Venus, which are very different environments from giant planets such as Jupiter and Saturn, in the same way as any planetary atmosphere is a very different environment from a comet or the ISM.

It is also important to quantify what constitutes a significant source of a given molecule while evaluating their abiotic versus biotic production mechanisms. We take $CH_3OH$, methanol, as an example. In their Table S2, S. Seager et al. (2025) state that there are no known significant abiotic sources of $CH_3OH$ on terrestrial planets. However, abiotic mechanisms contribute a nonnegligible (>10%) fraction of the total production rate of $CH_3OH$ on Earth (M. A. H. Khan et al. 2014; K. H. Bates et al. 2021). At a minimum, this is 20 times higher as a fractional contribution than existing experiments for DMS in a gas mixture similar to the atmosphere of K2-18 b. Thus, the classification of DMS versus $CH_3OH$ under the criterion of "No Known Significant False Positives (Context)" in S. Seager et al. (2025; Table 1) appears inconsistent. Overall, it is important that any standard of assessment adopted for biosignatures is applied uniformly across all candidate biosignature molecules.

## 3. Methods

In this work we perform a wide array of atmospheric retrievals on the JWST transmission spectrum of K2-18 b in the 0.8–12 $\mu$m range using a number of atmospheric retrieval frameworks. This sub-Neptune (B. T. Montet et al. 2015; R. Cloutier et al. 2019) has a mass of $8.63 \pm 1.35\,M_\oplus$ and a radius of $2.61 \pm 0.09\,R_\oplus$ (R. Cloutier et al. 2019; B. Benneke et al. 2019). Its transit was observed three times with JWST, once with each of NIRISS SOSS, NIRSpec G395H, and MIRI LRS. These observations led to $\gtrsim 3\sigma$ inferences of $CO_2$, $CH_4$ (M23), and DMS and/or DMDS (M25). The inferences of $CO_2$ and $CH_4$ and nondetections of other species such as

**Table 1**
Values of $\ln B$ against the Baseline $CH_4 + CO_2$ Model for Promising Candidates in Both MIRI Datasets.

| Species | VIRA | | pRT | | POSEIDON | |
|---|---|---|---|---|---|---|
| | JExoRES | JexoPipe | JExoRES | JexoPipe | JExoRES | JexoPipe |
| Chloroethane | 3.5 | 4.4 | 3.3 | 4.2 | 3.1 | 4.0 |
| Propyne | 3.1 | 3.1 | 2.3 | 2.7 | 2.6 | 2.7 |
| Dichloromethane | 2.7 | 2.9 | 2.0 | 2.6 | 2.6 | 2.8 |
| Methacrylonitrile | 2.7 | 2.6 | 2.6 | 2.7 | 2.6 | 2.4 |
| Bromoethane | 2.9 | 2.2 | 2.5 | 2.0 | 2.6 | 2.0 |
| Cyclohexane | 2.7 | 3.0 | 1.6 | 2.1 | 2.5 | 3.0 |
| Butane | 2.6 | 2.4 | 2.4 | 2.4 | 2.5 | 2.1 |
| Cyclopentane | 2.3 | 2.1 | 2.0 | 2.1 | 2.4 | 2.2 |
| DMS | 2.6 | 2.8 | 2.0 | 2.5 | 2.2 | 2.5 |
| Allyl chloride | 2.3 | 2.6 | 1.9 | 2.0 | 2.1 | 2.1 |
| DMDS | 3.5 | 3.0 | 1.8 | 1.9 | 2.3 | 1.9 |

**Note.** Natural log Bayes factors obtained from petitRADTRANS, VIRA, and POSEIDON for the 10 molecules which reach the $\ln B = 2.0$ threshold in the POSEIDON retrievals using both JExoRES and JexoPipe MIRI datasets, as well as for dimethyl disulfide, found at $\ln B \geqslant 2.5$ in both MIRI datasets by N. Madhusudhan et al. (2025). Typical uncertainties on $\ln B$ are $\sim\pm 0.5$. As a guide, the T. Sellke et al. (2001) and R. Trotta (2008) conversion yields $\ln B = 1.0 \Leftrightarrow 2.0\sigma$, $\ln B = 2.0 \Leftrightarrow 2.5\sigma$ and $\ln B = 3.0 \Leftrightarrow 3.0\sigma$.

$NH_3$, $H_2O$, and CO led to its classification as a possible hycean world (N. Madhusudhan et al. 2021).

The inference of DMS and/or DMDS, potential biosignatures (S. D. Domagal-Goldman et al. 2011; S. Seager et al. 2013; D. C. Catling et al. 2018; E. W. Schwieterman et al. 2018; S.-M. Tsai et al. 2024), led to the suggestion of possible biological activity on the planet (M25). However, as discussed in M25, it is important to consider if there are other species that may contribute to the features attributed to DMS and/or DMDS. This possibility was explored by W26, who, having considered 90 hydrocarbons, found that three of them resulted in Bayes factors $\ln B \geqslant 2.5$ in both the M25 MIRI JExoRES and JexoPipe data, comparable to that obtained for DMS and/or DMDS. However, the exploration of W26 focused only on the MIRI observations. Therefore, the robustness of their findings was not assessed against the NIR data reported in M23.

In the present work, we conduct a very broad search for chemical species in the atmosphere of K2-18 b. Furthermore, our search is agnostic, in the sense that we make no prior assumptions as to the theoretical plausibility of any specific chemical species being present in the atmosphere of K2-18 b. Indeed, we consider a list of 661 species, including nearly all those present in the HITRAN cross-section database, several of which are unlikely to be present in the atmosphere of K2-18 b based on present understanding of chemical and physical processes. We then investigate any model preference for them across all the data available. We first systematically investigate whether the MIRI JExoRES and JexoPipe datasets provide support for their presence in the atmosphere of K2-18 b. For those for which at least moderate model preference is consistently found, we then verify whether this is supported also by the NIR data presented in M23, considered independently as a separate follow-up step. We consider as promising candidates the species which are highest ranked under our workflow, reaching noteworthy preference across all datasets considered independently. However, we note that in this initial work we do not account for the effect of the multiplicity problem, as we discuss further in Section 6. Previous retrievals on these datasets in M25 and W26 were carried out with the AURA retrieval code and its variant Aurora. For robustness in the present work, we carry out the majority of our retrievals with the retrieval code POSEIDON (R. J. MacDonald & N. Madhusudhan 2017; R. J. MacDonald 2023). However, in order to ensure our results are independent of the retrieval framework used, we perform multiple cross checks of promising species with two other independent retrieval codes, petitRADTRANS (pRT, P. Mollière et al. 2019; E. Nasedkin et al. 2024) and VIRA (S. Constantinou & N. Madhusudhan 2024).

### 3.1. Observations

We consider JWST observations of K2-18 b in total spanning a wavelength range between $\sim$0.8–12 $\mu$m taken as part of JWST GO Program 2722 (PI: N. Madhusudhan). For the present analysis, we first consider observations between $\sim$5 and 12 $\mu$m taken with JWST MIRI (S. Kendrew et al. 2015; J. Bouwman et al. 2023) and presented by M25. The observations took place on 2024 April 25–26 over 5.85 hr, with the primary transit itself taking 2.68 hr. For the present work we consider both the JExoRES and JexoPipe reductions of the above MIRI observation. M25 considered different binning prescriptions and found the spectrum to be consistent between them. In this work, we use the nominal binning case of M25, where the native-resolution spectrum was binned to a width of 0.2 $\mu$m or 5 pixels, whichever contained the most pixels. This prescription resulted in reduced $\chi^2$ values of 1.06 and 1.16 with a flat line fit for JExoRES and JexoPipe, respectively. We note that the value of the reduced $\chi^2$ is known to depend on the binning prescriptions adopted, and does not take into account the wavelength distribution of residuals. For these and other reasons, its usage to assess model fits to exoplanet spectra is generally discouraged (e.g., L. Welbanks et al. 2023).

We also consider observations with NIRISS (R. Doyon et al. 2012), spanning a wavelength range of $\sim$0.8–2.8 $\mu$m, combined with NIRSpec G395H (P. Ferruit et al. 2012; S. M. Birkmann et al. 2014) observations encompassing the $\sim$3–5 $\mu$m range, as presented by M23. The NIRSpec G395H observations were taken on 2023 January 20–21 with a total observing time of 5.3 hr, while the NIRISS observations were made on 2023 June 1 over a span of 4.9 hr, each observing one primary transit of K2-18 b. The resulting spectra, as presented

in M23, were binned at 2 pixels bin$^{-1}$ for NIRISS, while being kept at the native (1 pixel) resolution for NIRSpec.

### 3.2. Retrieval Setup

We carry out a retrieval analysis of the above data following the approach of M25, in order to investigate the model preferences for a wide array of molecules. We specifically consider three independent retrieval frameworks: VIRA (S. Constantinou & N. Madhusudhan 2024), pRT (P. Mollière et al. 2019; E. Nasedkin et al. 2024), and POSEIDON (R. J. MacDonald & N. Madhusudhan 2017; R. J. MacDonald 2023). We note that VIRA is the latest development of the same family of retrieval codes as the Aurora retrievals used by W26 and the AURA retrievals used in M25. On the other hand, POSEIDON was developed independently and does not share the same architecture as the AURA family of retrieval codes. All three retrieval codes model the terminator atmosphere as a 1D column in hydrostatic equilibrium with uniform chemical abundances and a parametric $P$–$T$ profile (N. Madhusudhan & S. Seager 2009). Each retrieval code uses pyMultiNest (F. Feroz et al. 2009; J. Buchner et al. 2014) for parameter estimation. We have found this to be robust for the dimensionality of the retrievals in this work across different choices for numbers of live points and sampling efficiencies. We compute our forward models at average resolving powers of $R \sim 15{,}000$ for the NIR and $R \sim 8000$ for the MIR. Our choice is informed by previous work (e.g., L. Felix et al. 2025) showing that using higher-resolution models (e.g., T. G. Beatty et al. 2024; A. Bello-Arufe et al. 2025; E.-M. Ahrer et al. 2025) does not have a significant impact on the retrieval results. We give our forward model specifications, as well as the settings adopted for other retrieval parameters, in Table 6 in Appendix A. The mixing ratios of molecular species beyond $H_2$ and He are treated as independent free parameters, with log-uniform priors. A schematic for our framework is shown in Figure 1.

#### 3.2.1. Species Selection

We carry out a wide-ranging and agnostic analysis of the MIRI (M25) and NIRISS NIRSpec (M23) data for K2-18 b. As shown in Figure 1, we first conduct a search for 661 species in the MIRI data, using an extension of POSEIDON enabling sequential retrievals. We run retrievals on both the JExoRES and JexoPipe datasets. We then identify the species for which a natural log Bayes factor $\ln B \geqslant 2.0$ is obtained from both the JExoRES and the JexoPipe MIRI data. We note that the standard for moderate evidence in R. Trotta (2008) is indicated as $\ln B \geqslant 2.5$. However, this does not consider the presence of uncertainties in the estimation of $\ln B$, due to both random and systematic effects, e.g., due to the use of different retrieval codes. We estimate that this uncertainty can result in variations up to $\ln B \sim 0.5$. We note that this value corresponds to the average range spanned by the $\ln B$ values obtained for any given species and dataset through different retrieval codes, reported in Tables 1 and 2. As our aim is to identify all candidate species which may be able to explain the excess absorption in the spectrum of K2-18 b, in order to be conservative, we pose our threshold for potential moderate evidence at $\ln B = 2.0$. For the set of species crossing this threshold with POSEIDON, we then verify whether $\ln B \geqslant 2.0$ model preference is also obtained in retrievals with pRT and VIRA. We thus obtain a restricted set of candidate species which reach the $\ln B \geqslant 2.0$ threshold across all pipelines and retrieval codes considered. For each of these, we then carry out similar retrievals with each of VIRA, pRT, and POSEIDON on the NIR dataset at native resolution, and again we identify the species which appear promising in the NIR dataset.

#### 3.2.2. Model Specification

In order to explore model preferences for the 661 species, we build a canonical model for each. Following the approach developed in M25, and later replicated in W26, we define the canonical model for chemical constituent X as containing three chemical constituents: $CH_4$, $CO_2$, and X, where X is any species or combination of species for which the model preference is to be derived. In M25, canonical models were constructed where X was considered to be DMS, or DMDS, or the combination of DMS and DMDS. In W26, the set of explored species was expanded, letting X be any of 90 molecules considered. In the present study, X is any of the 661 species considered. The model preference values reported are with respect to the baseline model only including $CO_2$ and $CH_4$. We quote model preference as the natural logarithm of the Bayes factor ($\ln B$).

The 661 species, listed in Appendix B, include all those present in the opacity database originally built into POSEIDON and available from its repository, as well as most of the HITRAN (I. E. Gordon et al. 2022) cross-section database, including species from all categories listed therein. When available, we adopt the cross sections at $T \approx 300$ K and $P \approx 1$ bar; otherwise, we use cross sections for the closest available temperature. We excluded species for which no opacity data were available in the MIR, or, as in the case of formaldehyde, they were available only for very high temperatures ($T = 998$ K). Furthermore, three hydrofluoroethers whose molecular weights we were not able to independently verify were also excluded. We thus obtained our final set of 661 species. For wavelength regions not covered by the available cross-section data, we assume no opacity from the relevant absorber. The pressure, temperature and wavelength range for each cross section obtained from HITRAN is reported in Table 8 in Appendix B for those species resulting in noteworthy model preferences.

For all our retrievals, we adopt the N. Madhusudhan & S. Seager (2009) pressure–temperature profile, like M25 and W26 do, which introduces six free parameters to our retrievals. We also allow for patchy clouds and hazes, following the R. J. MacDonald & N. Madhusudhan (2017) and A. Pinhas et al. (2019) parameterization. This includes four free parameters: the cloud-top pressure $P_c$ for the cloud deck; the Rayleigh enhancement factor $a$ and wavelength dependence $\gamma$ (such that the scattering cross section $\sigma$ depends on wavelength $\lambda$ as $\sigma \sim a\lambda^{\gamma}$) for the hazes, with $a = 1$ and $\gamma = -4$ corresponding to Rayleigh scattering; and a fractional cloud and haze coverage parameter $\phi$, with $\phi = 0$ indicating a fully clear atmosphere, and $\phi = 1$ a uniformly cloudy or hazy one. Finally, we include a free reference pressure $P_{ref}$, i.e., the pressure to which the white-light radius ($R_p = 2.61\,R_\oplus$) corresponds. This leads to 11 free parameters, plus the three molecular mixing ratios, for a total of 14 free parameters in most canonical model POSEIDON retrievals. This grows to 15

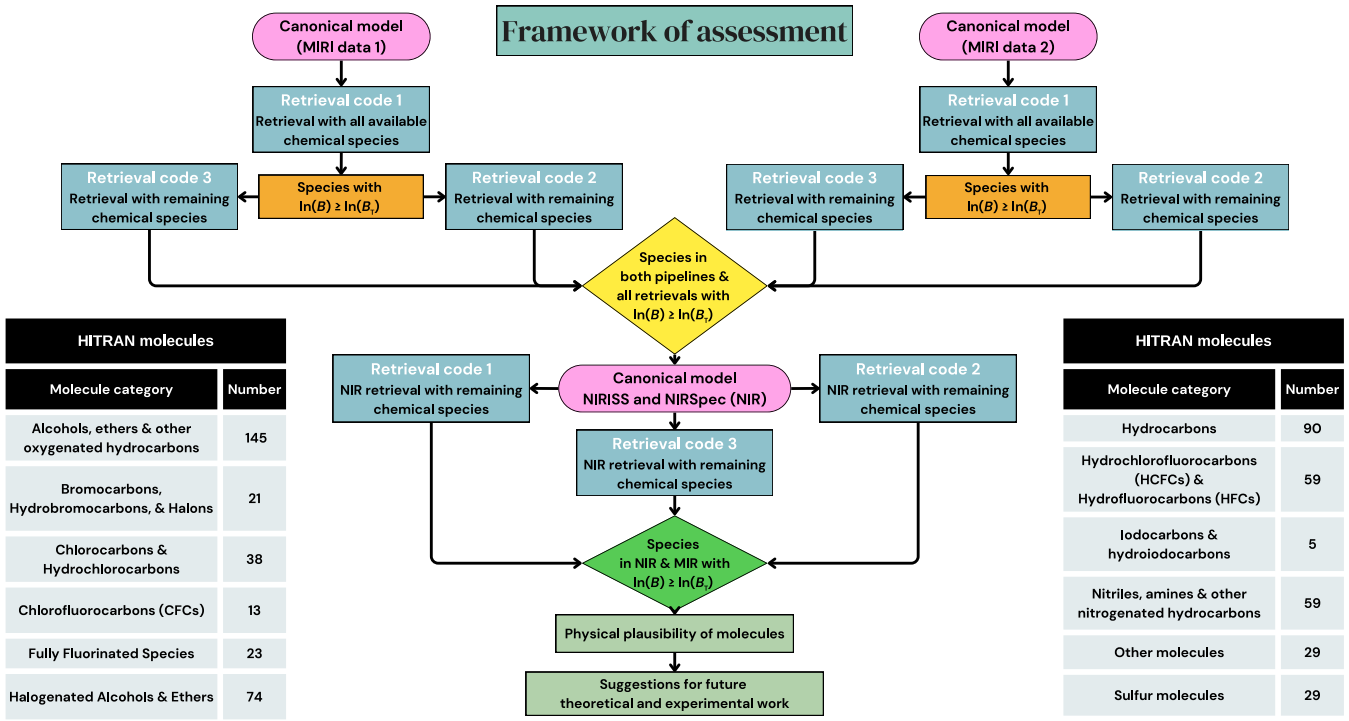



**Figure 1.** The flowchart shows our framework of assessment for possible molecules in the atmosphere of K2-18 b. Based on the inference of carbon dioxide ($CO_2$) and methane ($CH_4$) in the atmosphere of K2-18 b (M23), retrievals adopting canonical models are carried out following M25, assuming hydrogen-dominated atmospheres and including the mixing ratios of $CO_2$, $CH_4$, and X as free parameters, with X in this work being any of 661 species explored. The evidence for X is then computed by performing a Bayesian comparison between the relevant canonical model and a nested baseline model, with only X removed. Several independent retrieval codes can be used to increase the reliability of such a framework. In this work, retrieval codes 1, 2, and 3 are `POSEIDON`, `VIRA`, and `pRT`, respectively. Retrievals were initially performed with the `POSEIDON` retrieval code on the two available MIRI datasets for K2-18 b, resulting from the `JExoRES` and `JexoPipe` data reduction pipelines (MIRI data 1 and 2, in the pink curved boxes at the top left and top right). Nearly all molecules in the HITRAN cross-section database were used in these initial retrievals, as shown in the tables on the lower left- and lower right-hand sides of the figure. Additionally, some other available molecules, as well as atoms and ions, were considered, where originally included in `POSEIDON`. A threshold Bayes factor $\ln B_T$ is chosen, and chemical species for which $\ln B \geqslant \ln B_T$ is found are identified (orange rectangles), and follow-up retrievals are performed with `VIRA` and `pRT`. Chemical species for which $\ln B \geqslant \ln B_T$ is found across both reduction pipelines and all three retrieval frameworks (yellow diamond) are passed to the next step, where we include them in atmospheric retrievals on the NIR data from the `NIRISS` and `NIRSpec` JWST transits (pink curved box in the middle) of K2-18 b (M23). Finally, retrievals with `VIRA`, `pRT`, and `POSEIDON` are used to find if there are species for which $\ln B \geqslant \ln B_T$ can be reached in the NIR data (green diamond). We then discuss the physical plausibility of promising species being present in the atmosphere of K2-18 b. In this work, we chose $\ln B_T = 2.0$. This is informed by the threshold $\ln B = 2.5$ for moderate evidence proposed by R. Trotta (2008), and accounting for possible systematic uncertainties of up to $\pm 0.5$ on the estimation of $\ln B$, as discussed in Section 3.2.1.

free parameters when considering the NIR data and allowing for an offset between the NIRSpec and the NIRISS datasets. We show our model specifications and retrieval settings in Table 6 and our priors Table 7, both in Appendix A. As `pRT` works with mass mixing ratios rather than volume ones, we choose a prior $\mathcal{U}(-11, -0.1)$ to better reflect, in a low-mean molecular weight atmosphere, the $\mathcal{U}(-12, -0.3)$ prior in volume mixing ratios used in the `POSEIDON` and `VIRA` retrievals.

## 4. Results

In this work we performed a systematic search for the spectral signatures of 661 species in the atmosphere of exoplanet K2-18 b, using the three published datasets: the M25 `JExoRES` and `JexoPipe` data instances for the MIRI LRS spectrum, and the M23 NIRISS NIRSpec spectrum. We first explored which molecules the MIRI spectrum may be showing moderate (or stronger) evidence for, and then investigated if such evidence may also be present in the NIR range. In this section, we describe the outcome of this process. We start by considering the results obtained from the MIRI `JExoRES` dataset. We then compare these results with those obtained from the MIRI `JexoPipe` dataset, and as the final step in our workflow we search for the most promising species in the NIR dataset.

### 4.1. Canonical Retrievals With MIRI `JExoRES` Data

We begin by considering the MIRI `JExoRES` data. We first ensure consistency of our framework with established results by reproducing the key findings from M25 and W26. We then expand our search to a list of 661 species.

#### 4.1.1. Reproduction of Previous Work

M25 reported $\sim 3\sigma$ evidence, corresponding to $\ln B = 2.85$–$4.22$, for DMS and/or DMDS, when using the canonical model approach, i.e., comparing a model only including $CH_4$ and $CO_2$ with one also including either DMS, or DMDS, or both at the same time. This was reproduced by W26. We note that M25 used the `AURA` retrieval framework (A. Pinhas et al. 2018), and W26 used `Aurora` (L. Welbanks & N. Madhusudhan 2021; M. C. Nixon et al. 2024). Both codes belong to the `AURA` family, sharing many of the core components, and were developed in the same research group, so the agreement is

**Table 2**
Bayes Factors $\ln B$ in the Near-infrared for the 11 Species Reported in Table 1, Relative to a $CH_4 + CO_2$ Model

| Species | No Offset | | | One Offset | | |
|---|---|---|---|---|---|---|
| | VIRA | pRT | POSEIDON | VIRA | pRT | POSEIDON |
| DMS | 2.9 | 2.8 | 3.0 | 0.5 | 0.4 | 0.8 |
| Methacrylonitrile | 2.5 | 1.9 | 2.0 | 0.8 | 1.0 | 0.8 |
| Allyl Chloride | 2.2 | 1.4 | 1.8 | 0.4 | 0.2 | 0.6 |
| Butane | 1.0 | 0.5 | 0.9 | −0.3 | −0.6 | −0.2 |
| Bromoethane | 0.8 | 0.6 | 0.3 | −0.1 | −0.3 | 0.0 |
| Cyclopentane | 0.6 | 0.6 | 0.2 | −0.3 | 0.0 | −0.4 |
| Cyclohexane | 0.4 | 0.6 | 0.4 | −0.4 | −0.1 | −0.5 |
| Chloroethane | 0.2 | −0.1 | −0.1 | −0.4 | −0.2 | −0.1 |
| Propyne | 0.1 | 0.9 | 0.7 | −0.4 | −0.2 | −0.4 |
| Dichloromethane | 0.0 | −0.4 | −0.1 | 0.0 | −0.1 | −0.4 |
| DMDS | 0.7 | 1.0 | 0.8 | −0.3 | −0.1 | 0.0 |

**Note.** Typical uncertainties on $\ln B$ are $\sim\pm0.5$. As a guide, the T. Sellke et al. (2001) and R. Trotta (2008) conversion yields $\ln B = 1.0 \Leftrightarrow 2.0\sigma$, $\ln B = 2.0 \Leftrightarrow 2.5\sigma$, and $\ln B = 3.0 \Leftrightarrow 3.0\sigma$.

expected. Here, we reproduce the M25 results for the model preferences for DMS and/or DMDS with three independent codes, POSEIDON (R. J. MacDonald & N. Madhusudhan 2017; R. J. MacDonald 2023), pRT (P. Mollière et al. 2019; E. Nasedkin et al. 2024), and VIRA (S. Constantinou & N. Madhusudhan 2024), the latter of which also belongs to the AURA retrieval codes family, being its latest version. As shown in Table 1, generally consistent results are obtained across the three retrieval codes considered in this study, which are in turn consistent with the results reported by M25 and W26. We also consider the three additional species that, according to W26, result, with both the JExoRES and JexoPipe data, in Bayes factors $\ln B \geqslant 2.5$, which, according to Jeffreys' scale (see, e.g., R. Trotta 2008), corresponds to the minimum threshold for moderate evidence. For these three species as well, we perform consistency checks with the three abovementioned codes, also finding overall good agreement with the W26 results.

#### 4.1.2. Exploration of Additional Species

We conduct a broad exploration of additional chemical species in search of those that may explain the features in the MIRI LRS data besides DMS and/or DMDS, reported in M25. W26 considered 90 species in addition to DMS and DMDS, focusing on hydrocarbons. We now significantly expand upon the M25 and W26 work, considering nearly all species for which cross sections are available in the HITRAN database. In particular, we consider 556 species across the following classes: hydrocarbons; nitriles, amines, and other nitrogenated hydrocarbons; sulfur-containing species; alcohols, ethers, and other oxygenated hydrocarbons; bromocarbons, hydrobromocarbons, and halons; chlorocarbons and hydrochlorocarbons; chlorofluorocarbons (CFCs); fully fluorinated species; halogenated alcohols and ethers; hydrochlorofluorocarbons (HCFCs); hydrofluorocarbons (HFCs); and iodocarbons and hydroiodocarbons. We also include an additional 29 species belonging to other classes, as well as a further 76 originally considered in POSEIDON. Overall, our final database includes a total of 661 species.

The model preference values for the species resulting in $\ln B \geqslant 1.15$ are reported in Table 8 in Appendix B, and all remaining species are listed in Appendix B.1. We find that 15 of these are preferred by the JExoRES data at $\ln B \geqslant 2.0$ over a model only including $CH_4$ and $CO_2$. As mentioned above, our choice of $\ln B = 2.0$ as a threshold is due to this corresponding to the standard for moderate evidence in Jeffreys' scale, when accounting for a typical uncertainty of up to $\Delta \ln B = \pm 0.5$ in the estimation of the evidence. We note, however, that not all of these 15 molecules are known to have abiotic sources on Earth or beyond, with several being primarily biogenic or anthropogenic. We show a contribution plot in the MIR range including some of these species in Figure 2.

Among these 15 molecules, most result in Bayes factors comparable to DMS, spanning a range in $\ln B$ of one. However, it is possible that some of these species may only be preferred by the data from the JExoRES pipeline, and not by the JexoPipe one. Hence, we next proceed to perform the same retrievals on the JexoPipe data, in order to ascertain which species could be reliable substitutes for DMS and/or DMDS to explain the observed MIR features.

### 4.2. Canonical Retrievals with MIRI JexoPipe Data

As mentioned above, in order to reach robust conclusions, it is important to check that potential evidence for any molecule is not an artifact of a specific data reduction pipeline.

In order to achieve this additional level of robustness, here we compute the model preferences for each of 661 species we considered for JExoRES with the JexoPipe data as well. For species resulting in $\ln B \geqslant 1.15$, we report the results in Table 8 in Appendix B. We find that, as for JExoRES, 15 species result in natural log Bayes factors $\geqslant 2.0$ over $CH_4$ and $CO_2$ only. Five of these had been found at $\ln B < 2.0$ in the JExoRES dataset: tetramethylsilane (at $\ln B = 1.6$ in JExoRES), dimethyl carbonate ($\ln B = 1.5$), ethanethiol ($\ln B = 1.4$), 1-chloropentane ($\ln B = 1.2$), and dichloromethylphosphine ($\ln B = 1.0$). On the other hand, of those for which $\ln B \geqslant 2.0$ was obtained with the JExoRES dataset, the five that were not found with the JexoPipe spectrum are DMDS ($\ln B = 1.9$ with JexoPipe), methacryloyl chloride and methacrolein (both at $\ln B = 1.3$ with JexoPipe), trans-2-pentene ($\ln B = 1.1$), and 2-butene ($\ln B = 0.8$). We show the median retrieved spectra for DMS and methacrylonitrile in Figure 3.

Overall, 10 species reach the $\ln B = 2.0$ threshold in both datasets. These are chloroethane, bromoethane, propyne, methacrylonitrile, dichloromethane, cyclohexane, butane,

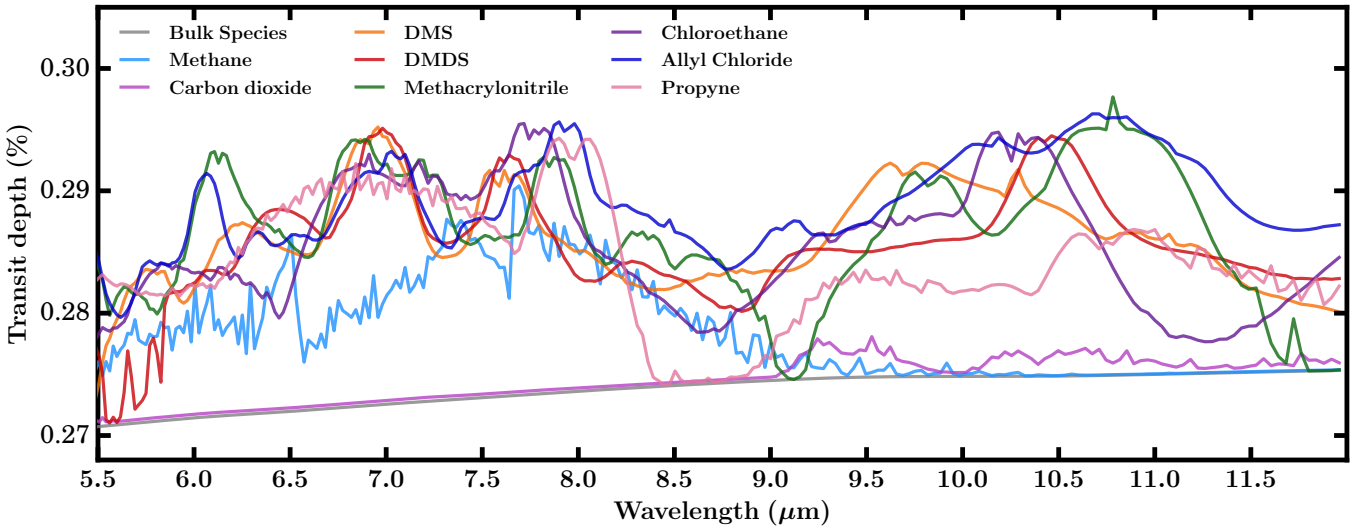



**Figure 2.** Contributions of molecules in the JWST MIRI range for the transmission spectrum of K2-18 b, assuming 1% $CO_2$ and $CH_4$, and $10^{-4}$ by volume for each of DMS, DMDS, methacrylonitrile, chloroethane, allyl chloride, and propyne.

cyclopentane, DMS, and allyl chloride. For these 10 species, we perform a robustness check with the two additional retrieval codes `pRT` and `VIRA`, for both `JExoRES` and `JexoPipe` data, shown in Table 1. We find that eight species are confirmed to have preference $\ln B \geqslant 2.0$ in all sets of retrievals, the exceptions being allyl chloride and cyclohexane. This leads to a final set of eight molecules for which at least moderate evidence may consistently be inferred in the MIR. The abundances found through `VIRA` and `POSEIDON` for these species are reported in Table 3, and the `POSEIDON` posterior distributions for a subset of these are shown in Figure 4.

### 4.3. Canonical Retrievals with Near-infrared Data

An NIR spectrum is also available for K2-18 b, obtained with the JWST NIRISS SOSS and NIRSpec G395H instruments (M23). Any claim of evidence for a trace species, such as DMS, should be verified with multiple lines of evidence, e.g., with different observations or different instruments. This has so far only been the case for DMS, for which M23 find model preferences of up to $2.4\sigma$ ($\ln B = 1.7$), in their no-offset scenario, but below $2\sigma$ ($\ln B < 0.9$) in the one-offset case. R. Hu et al. (2025) later confirmed that model preferences for DMS of up to $2.7\sigma$ ($\ln B = 2.3$) over a model only including six standard CNO species ($CH_4$, $CO_2$, CO, $NH_3$, HCN, and $H_2O$) can be obtained in the NIR, including offsets between all considered detectors.

For consistency with the approach we adopted with the MIRI observations, we here adopt the same canonical model configuration as in M25, W26, and our Sections 4.1 and 4.2, containing three chemical constituents: $CH_4$, $CO_2$, and X, where X is the species for which the model preference is to be derived. The model preference values we quote will hence be for these canonical models against a base model only including $CH_4$ and $CO_2$. Furthermore, as the motivation to search for DMS in the atmosphere of K2-18 b was originally the result of a potential inference of it in the no-offset scenario, we adopt no offsets at first here too, to verify if such a possibility exists for other species. As simpler models generally lead to increased evidence, the values in this work should be considered upper bounds on the evidence provided by the NIR data for each considered species.

We thus proceed to verifying which of the eight species for which the $\ln B = 2.0$ threshold was consistently cleared in the MIR data are also supported by the NIR data. Additionally, we also verify whether the NIR data provide support for the two species identified at $\ln B \geqslant 2.5$ in both MIRI `JExoRES` and `JexoPipe` datasets by W26 or M25 for which we do not consistently find $\ln B \geqslant 2.0$ when considering the two MIR datasets and three retrieval codes: cyclohexane and DMDS. For completeness, we also include allyl chloride in our NIR analysis, to avoid it being the only species from Table 1 excluded from this analysis. This leads to a total of 11 species to be verified against the NIR data.

We carry out atmospheric retrievals on this set of species using `VIRA`, `pRT`, and `POSEIDON`. We show the obtained model preference values in Table 2, finding that only one of the molecules is supported at $\ln B \geqslant 2.0$ in the NIR data across all three codes, DMS ($\ln B = 2.8$–$3.0$). One more species, methacrylonitrile, clears the $\ln B \geqslant 2.0$ threshold with `VIRA` and `POSEIDON`, but not with `pRT`, and another, allyl chloride, only does so with `VIRA`.

DMS, thus, is the only species for which our workflow yields $\ln B \geqslant 2.0$ across all considered datasets, i.e., two datasets corresponding to independent reductions of the M25 MIRI LRS spectrum and one corresponding to the M23 NIR spectrum, and with all retrieval frameworks used.

As discussed above, the significance values found here ought to be considered as upper bounds on the evidence for these species in the NIR, as considering more complex models can lead to lower evidence. For example, as reported in M23, when considering their preferred canonical model with one offset, the significance for DMS was $\sim 1\sigma$ compared to $2.4\sigma$ in the zero-offset case. Similarly, in our present retrievals, none of the molecules considered above reach a $\ln B = 2.0$ preference when allowing for an offset between the NIRISS and NIRSpec detectors.

### 4.4. Maximal Retrievals

Thus far, we have adopted a canonical model approach. This approach offers the significant benefit of allowing a fast and broad exploration of a wide set of chemical species (up to 661,

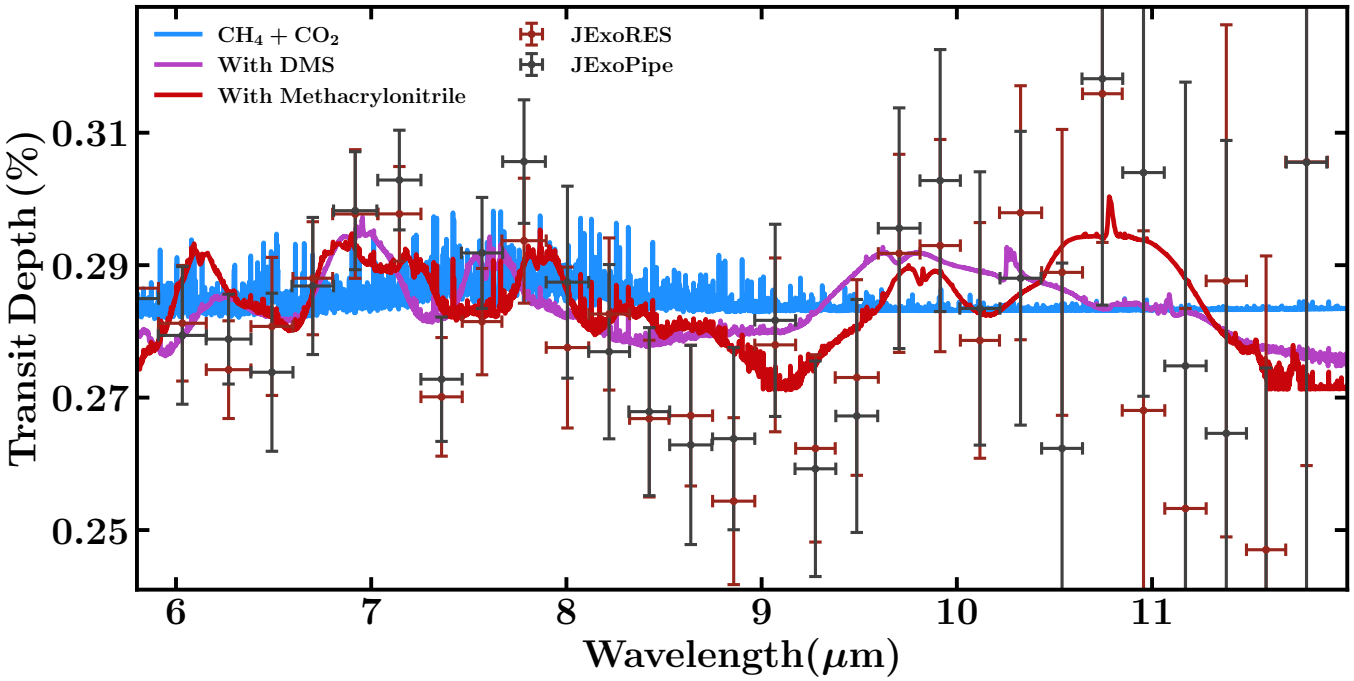



**Figure 3.** Retrieved spectra with the JWST MIRI `JexoPipe` data. The solid curves show median retrieved spectra obtained from the `POSEIDON` retrievals on MIRI `JexoPipe` data for the $CH_4 + CO_2$ baseline, and the canonical models for each of DMS and methacrylonitrile, the two species which are most preferred against the baseline model, when considering all cases described in this work. Also shown are the `JExoRES` and `JexoPipe` MIRI observations.

in this work). However, this comes at the expense of using a simple model, which in this case only contains two baseline chemical species ($CO_2$ and $CH_4$) in addition to the extra absorber which is investigated. This risks resulting in degeneracies between different absorbers being overlooked. Furthermore, if the baseline set of chemical species is incomplete, it may result in overestimating the detection significance for the extra absorber.

At the other end of the complexity spectrum are maximal model approaches (e.g., M25). These include a broader set of chemical species at once (as broad as 20, in M25), and as such they offer the benefit of exploring degeneracies between different absorbers, as well as the effects of including combinations of species. However, if the set of species considered is exceedingly broad, detection significances found through maximal models will be underestimated.

For completeness, we report here the results of maximal retrievals on all datasets considered in this study, carried out with `POSEIDON`. We verify the evidence for any species or set of species by comparing the maximal model to a nested model with the relevant absorber(s) removed, following the standard approach of B. Benneke & S. Seager 2013. For all retrievals, we preserve identical setups to those employed for the corresponding canonical models, the only change being the absorbers included.

#### 4.4.1. Mid-infrared

We consider a maximal setup including six CNO chemical species which may be expected in a hydrogen-rich temperate atmosphere ($CO_2$, $CH_4$, $H_2O$, CO, $NH_3$, and HCN) as well as the 11 species listed in Table 1. We first verify whether any model preference is present for excess absorption beyond $CH_4$ and $CO_2$, by removing all 15 remaining species. We find weak evidence toward this being the case with the `JExoRES` data, at $\ln B = 1.9$ (corresponding to $2.5\sigma$ using the conversion reported in T. Sellke et al. 2001; R. Trotta 2008; B. Benneke & S. Seager 2013), while moderate evidence ($\ln B = 2.2$, $2.6\sigma$) can be reached with `JexoPipe`. We note that in both cases this is lower than found with the most preferred canonical models, each including one species beyond $CH_4$ and $CO_2$. This is due to the complexity penalty introduced in calculating the Bayesian evidence ($\ln Z$), such that a maximal model including several degenerate species results in a lower evidence than a smaller model (e.g., a canonical one) which provides an equally good fit to the data.

The removal of the 11 species in Table 1 from the maximal model does not result in a meaningful change in model evidence when using the `JExoRES` data, with a Bayes factor in favor of the presence of those 11 species of $\ln B = 0.8$ ($1.9\sigma$). On the other hand, slightly higher significances are found when considering the `JexoPipe` data. In this case, we find weak evidence ($\ln B = 1.3$, $2.2\sigma$) toward the species listed in Table 1 being present.

#### 4.4.2. Near-infrared

We next perform a similar analysis with the NIR data. We begin with a no-offset case, consistent with the approach we adopted for the canonical model retrievals. In this case, our maximal model includes the six aforementioned CNO species ($CO_2$, $CH_4$, $H_2O$, CO, $NH_3$, and HCN), and the two species which the canonical model retrievals with `POSEIDON` revealed to be promising (DMS and methacrylonitrile). This maximal model is preferred at $\ln B = 3.2$ ($3.0\sigma$) over one only including the six CNO species. However, using the maximal model as a reference, only weak evidence ($\ln B = 1.3$, $2.2\sigma$) is found for DMS individually, and none is found for methacrylonitrile, indicating they are largely degenerate with each other.

When allowing for an offset, the above maximal model including the six standard CNO species ($CO_2$, $CH_4$, $H_2O$, CO, $NH_3$, and HCN), DMS, and methacrylonitrile results in weak

**Table 3**
Abundance Estimates for the 11 Species Listed in Table 1 Obtained With VIRA and POSEIDON Canonical Model Retrievals on the Three Datasets Considered in This Work

| Species | VIRA | | | | POSEIDON | | | |
|---|---|---|---|---|---|---|---|---|
| | MIR | | NIR | | MIR | | NIR | |
| | JExoRES | JexoPipe | No Offset | One Offset | JExoRES | JexoPipe | No Offset | One Offset |
| DMS | $-3.66^{+1.10}_{-1.42}$ | $-3.65^{+1.12}_{-1.33}$ | $-4.42^{+0.59}_{-0.61}$ | $<-4.15$ | $-4.20^{+1.03}_{-1.24}$ | $-3.83^{+0.92}_{-1.25}$ | $-4.18^{+0.60}_{-0.60}$ | $<-4.12$ |
| Methacrylonitrile | $-4.13^{+1.26}_{-1.24}$ | $-4.04^{+1.28}_{-1.30}$ | $-4.60^{+0.72}_{-0.70}$ | $<-4.24$ | $-4.44^{+1.01}_{-1.11}$ | $-4.34^{+1.03}_{-1.09}$ | $-4.28^{+0.83}_{-1.35}$ | $<-4.44$ |
| Allyl chloride | $-3.97^{+1.18}_{-1.48}$ | $-3.98^{+1.19}_{-1.37}$ | $-3.96^{+0.68}_{-0.69}$ | $<-3.63$ | $-4.58^{+1.13}_{-1.18}$ | $-4.06^{+0.94}_{-1.36}$ | $<-2.75$ | $<-3.82$ |
| Butane | $-3.68^{+1.21}_{-1.41}$ | $-3.37^{+1.11}_{-1.46}$ | $<-3.30$ | $<-5.17$ | $-4.02^{+1.02}_{-1.32}$ | $-3.92^{+1.08}_{-1.26}$ | $<-3.30$ | $<-5.42$ |
| Bromoethane | $-3.56^{+1.03}_{-1.41}$ | $-3.64^{+1.15}_{-1.52}$ | $<-2.86$ | $<-4.72$ | $-3.92^{+0.97}_{-1.24}$ | $-3.89^{+1.11}_{-1.60}$ | $<-2.92$ | $<-5.13$ |
| Cyclopentane | $-3.67^{+1.32}_{-1.35}$ | $-3.32^{+1.27}_{-1.48}$ | $<-2.88$ | $<-5.16$ | $-3.91^{+1.10}_{-1.09}$ | $-3.55^{+1.10}_{-1.33}$ | $<-3.17$ | $<-5.44$ |
| Cyclohexane | $-2.28^{+0.84}_{-1.50}$ | $-2.11^{+0.73}_{-1.37}$ | $<-3.70$ | $<-5.73$ | $-2.93^{+1.02}_{-1.25}$ | $-2.39^{+0.78}_{-1.42}$ | $<-3.52$ | $<-5.86$ |
| Chloroethane | $-3.38^{+1.03}_{-1.29}$ | $-3.43^{+1.03}_{-1.36}$ | $<-3.42$ | $<-5.06$ | $-3.78^{+0.94}_{-1.21}$ | $-3.97^{+0.97}_{-1.04}$ | $<-3.73$ | $<-5.53$ |
| Propyne | $-2.84^{+0.97}_{-1.29}$ | $-2.91^{+1.03}_{-1.36}$ | $<-4.14$ | $<-6.02$ | $-3.31^{+0.89}_{-1.39}$ | $-3.16^{+0.92}_{-1.26}$ | $<-4.29$ | $<-6.18$ |
| Dichloromethane | $-2.60^{+0.73}_{-1.09}$ | $-2.81^{+0.77}_{-1.08}$ | $<-2.87$ | $<-4.26$ | $-2.71^{+0.69}_{-1.20}$ | $-2.96^{+0.78}_{-1.12}$ | $<-3.15$ | $<-4.36$ |
| DMDS | $-3.35^{+1.00}_{-1.25}$ | $-3.40^{+1.10}_{-1.32}$ | $<-3.26$ | $<-4.82$ | $-4.46^{+1.06}_{-1.09}$ | $-4.45^{+1.10}_{-1.13}$ | $<-3.04$ | $<-4.74$ |

**Note.** When a dataset provides $\ln B \geqslant 2.0$ support for a species with the relevant retrieval code, the median retrieved abundance and $1\sigma$ error bars are reported; otherwise, the $2\sigma$ upper limit is indicated.

preference ($\ln B = 1.3$, $2.2\sigma$) over the model with the standard species only, while no statistically significant preference is found for either of DMS or methacyrlonitrile alone compared to the maximal model. We show the median retrieved spectrum for a one-offset model including the six standard CNO species as well as DMS, the species that is overall most preferred when considering our work in its entirety, in Figure 5.

### 4.5. Overall Significances

Overall, we find that, of 661 initial species, 15 crossed the $\ln B = 2.0$ threshold for model preference against each of the MIRI JExoRES and MIRI JexoPipe datasets, with POSEIDON. Of these, eight crossed the threshold in both MIR datasets with all of VIRA, pRT, and POSEIDON, and were further investigated in the NIR. Among these, only DMS reached the $\ln B = 2.0$ threshold in the NIR data with all three retrieval codes used, when considering no offsets between detectors.

Beyond the canonical model retrievals, where the baseline model was only $CH_4$ and $CO_2$, we also considered maximal model retrievals with POSEIDON, which overall confirmed the inferences from the canonical models. In particular, for the MIRI data, we adopted a maximal model with 17 species, including the six standard CNO species, i.e., $CH_4$, $CO_2$, $H_2O$, CO, $NH_3$, and HCN, as well as the 11 species listed in Table 1. We found that this model is somewhat preferred over the $CH_4$ and $CO_2$ baseline, at $\ln B = 1.9$ ($2.5\sigma$) with the JExoRES data and $\ln B = 2.2$ ($2.6\sigma$) with the JexoPipe data. Only when using the JexoPipe data, weak evidence ($\ln B = 1.3$, $2.2\sigma$) for the maximal model is also found against one including all six standard CNO species.

When considering the NIR data without offsets, we also find moderate preference for the presence of DMS and/or methacrylonitrile. In particular, a maximal model including these two species as well as the six CNO species was preferred at $\ln B = 3.2$ ($3.0\sigma$) over one only including the six expected CNO species. However, DMS and methacrylonitrile remained mostly degenerate, with only DMS resulting in some weak evidence when considered individually, using the maximal model as reference. When considering one offset between the NIRSpec and NIRISS instruments, only weak preference is found for DMS and/or methacrylonitrile. Specifically, a model also including these two species is preferred at $\ln B = 1.3$ ($2.2\sigma$) against one only including the six standard CNO species, and the degeneracy between the two species persisted.

We highlight that this analysis shows the potential of atmospheric retrievals. When used with appropriate robustness checks and across a few datasets, they allow an agnostic list of 661 candidate molecules to be reduced to just a handful of promising candidates. In this work, requiring Bayes factors compatible with moderate evidence in each of three datasets corresponding to two independent observations at different wavelengths, with three independent retrieval codes, has been sufficient to achieve this aim, but different works may require different specific choices to be made. We do note however that in this work we have only considered individual contributions from single molecules, and that a more exhaustive analysis in the future could consider combinations of multiple species that might be more favored than any species individually. Furthermore, as discussed in Section 4.4, while the canonical model retrievals are helpful in finding a few promising candidates, these candidates remain degenerate with each other, and, to a lesser extent, with other species. More observations are needed to be able to break this degeneracy. We show the spectra corresponding to the median results from the POSEIDON retrievals on the MIRI JexoPipe dataset for DMS and methacrylonitrile in Figure 3.

### 4.6. Estimated Abundances

As shown in Table 3, for most species for which moderate evidence is found in the MIR, we infer potential volume mixing ratios from the MIRI data between $\sim 10^{-3}$ and $10^{-4}$, consistent between the JExoRES and JexoPipe data instances. These values are similar to the abundances found for DMS and/or DMDS by M25. For the species which are also inferred with moderate evidence in the NIR with no offsets between detectors, we find overall lower ($\sim 10^{-5}$) median abundances, but still consistent at $1\sigma$ with the MIR results. This, too, is consistent with what was found for DMS

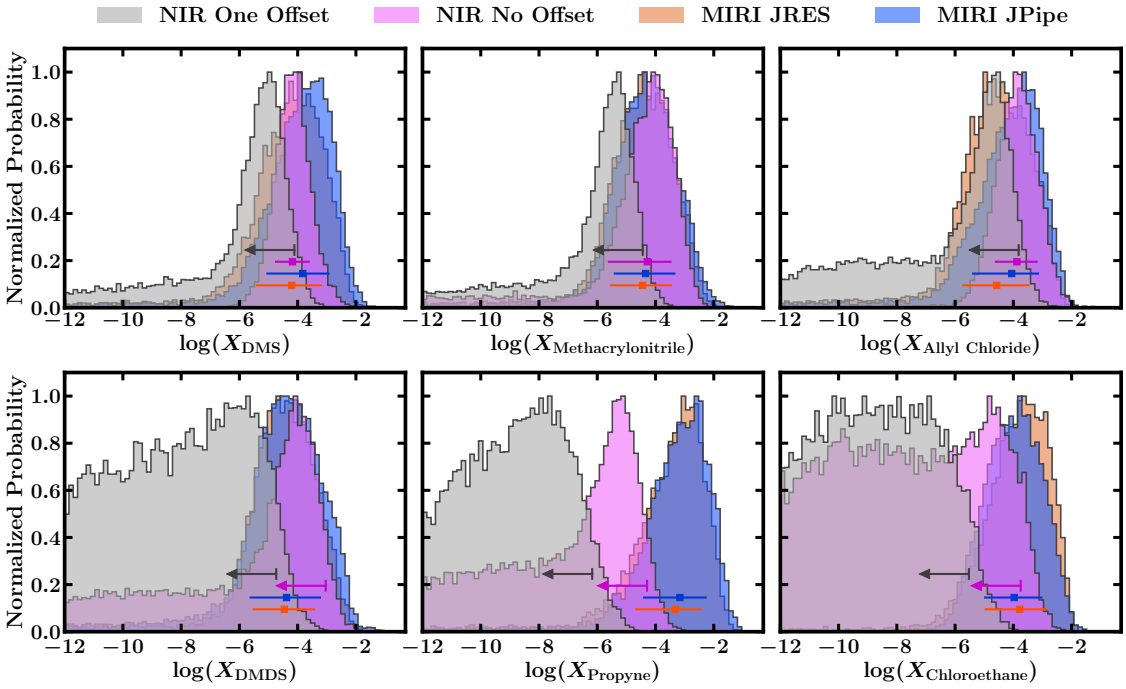



**Figure 4.** Posterior distributions for the volume mixing ratios of selected species, as obtained from the respective canonical model `POSEIDON` retrievals on the MIRI `JExoRES`, MIRI `JexoPipe`, and NIRISS NIRSpec spectra of K2-18 b.

in M23. Species for which no evidence is found in the NIR instead are found to have $2\sigma$ abundance upper limits of $\sim 10^{-3}$–$10^{-4}$, similar to the other nondetections reported in M23. We note that, in most of these cases, the $2\sigma$ upper limits in the NIR are consistent with the median retrieved abundances in the MIR. This implies that their nondetection in the NIR is not grounds to dismiss the possibility that they may be present in the atmosphere of K2-18 b. This caveat may also apply to other species, which, while potentially present, may lack features strong enough to allow their inference with the present data quality. This possibility is further discussed in Section 6. Posterior distributions for select species are shown in Figure 4.

## 5. Physical Plausibility of Results

Any inference of a chemical signature on an exoplanet needs to be assessed for its physical plausibility, in the context of the environment in which it is potentially inferred. Such a process requires an assessment of its chemical properties, as well as photochemical models that simulate atmospheric composition under a range of plausible conditions, taking into account the uncertainties in the stellar spectra, chemical reaction networks, transport, and albedo (G. J. Cooke & N. Madhusudhan 2024). When observed spectral features are attributed to molecules whose predicted abundances are orders of magnitude different from plausible theoretical expectations, this raises questions about the accuracy of either the observations or the models, or both. Such discrepancies could arise from retrieval degeneracies (e.g., M. R. Line & V. Parmentier 2016; L. Welbanks & N. Madhusudhan 2019, 2022; A. Lueber et al. 2024; A. Novais et al. 2025) and unknown opacity sources (e.g., P. Niraula et al. 2022, 2023), but they may also indicate that current chemical networks are incomplete, especially in parameter-space regimes where reaction pathways are missing or unconstrained.

In this section, we discuss a number of promising candidate species obtained. In particular, we begin by discussing DMS, which is the only species for which moderate model preference is found across all the MIRI and NIR zero-offset retrievals. We then also discuss methacrylonitrile and allyl chloride, for which the $\ln B = 2.0$ threshold for moderate preference is also reached in all our MIRI retrievals, as well as in the NIR with at least one retrieval code, for the no-offset case. Then, we consider three hydrocarbons that are in common with W26, who found them with significances $\ln B \geqslant 2.5$ with both of the MIRI datasets, `JExoRES` and `JexoPipe`. We summarize our results for DMS, methacrylonitrile and allyl chloride in Table 4, and for the other three hydrocarbons in Table 5.

### 5.1. Dimethyl Sulfide

The most promising species found in this work is DMS, $(CH_3)_2S$. This species is the most abundant biologically produced sulfur compound emitted to Earth's atmosphere (D. Simpson et al. 1999) with atmospheric mixing ratios of up to $\sim$1 ppbv, usually fluctuating between concentrations of 1–100 pptv (E. L. Mungall et al. 2016; S.-B. Yan et al. 2023). DMS is mainly produced as a byproduct of dimethylsulfoniopropionate (DMSP), which is generated by marine phytoplankton, including bacteria and algae (P. Liss et al. 1993; K. M. Ledyard & J. W. Dacey 1994; T. Groene 1995), although it can be produced without DMSP as a precursor (P. T. Visscher et al. 2003; O. Carrión et al. 2015).

DMS does have astrophysical sources, as it has been observed in a comet (N. Hänni et al. 2024) and in the ISM, at abundances relative to hydrogen of $\sim 1 \times 10^{-10}$ (M. Sanz-Novo et al. 2025). DMS is produced photochemically in laboratory experiments up to abundances of 0.6 ppmv when $CH_4$ and $H_2S$ are present without $CO_2$, with the DMS abundance reducing to 0.05 ppmv as $CO_2$ is increased to 0.1% by volume (N. W. Reed et al. 2024). There is, however, no evidence for $H_2S$ in the atmosphere of K2-

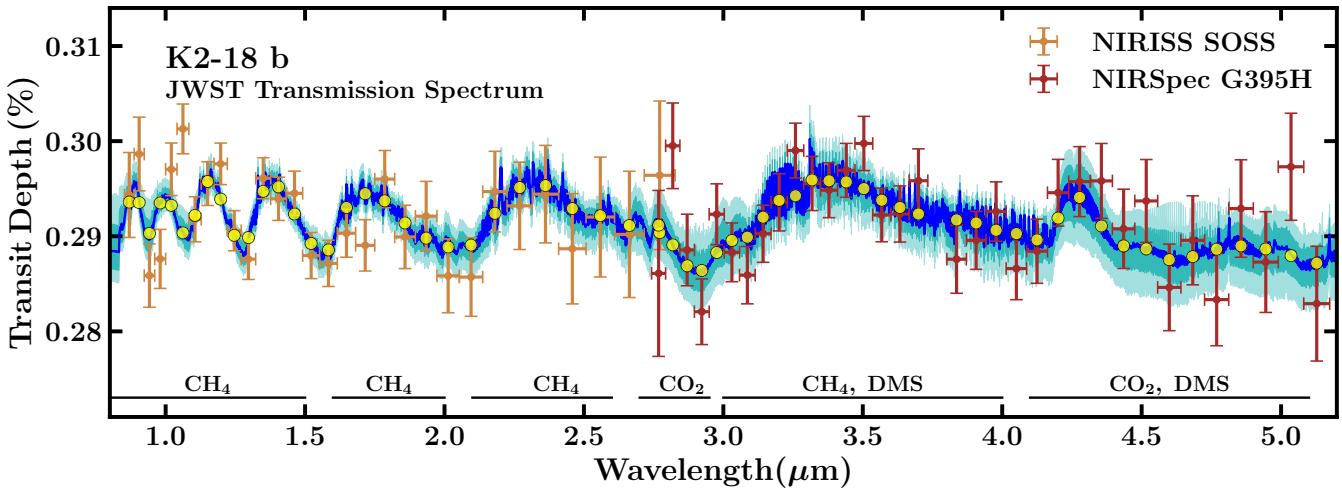



**Figure 5.** Median retrieved spectrum with `POSEIDON` (blue line) and $1\sigma$ and $2\sigma$ uncertainties (shaded regions) in the NIR for a model including six standard CNO species ($CO_2$, $CH_4$, $NH_3$, CO, HCN, and $H_2O$) and DMS, with one offset. The contributions of the various absorbers are shown in Figure 5 of M23 and Figure 3 of R. Hu et al. (2025)

18 b (W26; M25, R. Hu et al. 2025), and there is evidence for $CO_2$ existing alongside $CH_4$ (M23; R. Hu et al. 2025). Consequently, as cometary delivery of plentiful DMS to be sustained for billions of years is unfeasible (M25), and the ISM generates negligible abundances (M. Sanz-Novo et al. 2025), 0.05 ppmv of DMS is the current known upper limit on abiotic pathways for creating DMS in an environment similar to the conditions in the atmosphere of K2-18 b. This value is $\sim$4 dex lower than the median abundances found for DMS in M25, and $\sim$1 dex lower than that found with the less constraining NIR observations in the canonical model of M23. An alternative abiotic DMS pathway has been suggested by R. Hu et al. (2025), but this requires a deep atmosphere and adequate $H_2S$, which is not detected in the atmosphere of K2-18 b. The lack of $NH_3$ further argues against a deep atmosphere.

Determining whether DMS (if its presence is confirmed) emanates from a biotic source will require three criteria to be met: a stronger constraint on the atmospheric DMS abundance; an inference on whether K2-18 b is a hycean world or if it has a deep atmosphere with no liquid water ocean (which R. Hu et al. 2025 have further shown to be unlikely); and ruling out abiotic sources for the inferred abundance in the given context.

### 5.2. Methacrylonitrile and Allyl Chloride

As discussed in Section 4, the species coming closest to DMS in our analysis is methacrylonitrile ($C_4H_5N$, also known as methylacrylonitrile). This is also a trace chemical on Earth with no significant abundance in the atmosphere. It has been found to be toxic to mammals (U. Pozzani et al. 1968; M. Y. Farooqui & M. M. Mumtaz 1991). Its industrial use includes the production of polymers and as a chemical intermediary in the synthesis of other compounds (M. Y. Farooqui & M. M. Mumtaz 1991; N. Grassie & E. Vance 1956). While it has also not been observed in any other planetary atmosphere, it has recently been located in a molecular cloud at low abundances of $10^{-11}$ relative to $H_2$ (J. Cernicharo et al. 2022).

Lastly, the only other species resulting in our $\ln B \geqslant 2.0$ threshold being met in the NIR (no-offset case) with at least one of the retrieval codes we consider is allyl chloride. This molecule ($C_3H_5Cl$, also known as 3-Chloroprop-1-ene) is a neurotoxin, which can be produced from chlorination of propylene (A. Turja et al. 2011) and is used in chemical synthesis (A. R. Berger & H. H. Schaumburg 2005; W. Wang et al. 2014). It is relatively insoluble in water and, while it is a liquid at room temperature and pressure, it is volatile and could exist as a vapor (A. R. Berger & H. H. Schaumburg 2005) in the atmosphere of K2-18 b. Its abundance in Earth's atmosphere has not been reported globally and it has not been located in astrophysical sources.

### 5.3. Other Candidates

We now consider the plausibility of other candidate molecules. Specifically, we focus on the three hydrocarbons that are in common with those found in W26 with preference $\ln B \geqslant 2.5$ in both MIRI datasets. All these molecules were found by W26 to result in an $\ln B$ between 2.7 and 3.4 with both `JExoRES` and `JexoPipe` data, comparable to DMS, similar to the present work. These are propyne ($C_3H_4$), cyclohexane ($C_6H_{12}$), and butane ($C_4H_{10}$). We summarize the known abundances of these three molecules on Earth or in astrophysical environments in Table 5.

Propyne (also known as methylacetylene) is not present in Earth's atmosphere at significant abundances. It is emitted by some vehicles (M.-S. Kim et al. 2006; Y. Liu et al. 2008) and has been observed in some areas at concentrations $\lesssim$20 ppt (A. L. Steiner et al. 2008). It has been found in the atmospheres of all solar system giant planets (T. de Graauw et al. 1997; T. Fouchet et al. 2000; V. Meadows et al. 2006; M. Burgdorf et al. 2006), with abundances generally $\lesssim$10 ppbv, and that of Pluto at $\sim$1 ppmv (A. J. Steffl et al. 2020). A mixing ratio of 4 ppmv was measured by the Cassini Ion Neutral Mass Spectrometer (INMS) in Titan's atmosphere (J. H. Waite et al. 2005; C. A. Nixon et al. 2013). Propyne has also been observed in a prestellar core (C. Vastel et al. 2014), a protostar (I. Andron et al. 2018), and a protoplanetary disk (A. M. Arabhavi et al. 2024), as well as the ISM (L. E. Snyder & D. Buhl 1973). The abundances in these environments are lower than that in the atmosphere of Titan. While propyne clearly exists in nature, we do not detect it in the NIR in the retrievals we present here. W26 describe their propyne retrieval posterior with a peak near an abundance of $10^{-3}$, indicating relatively large abundances. We find a consistent

**Table 4**
Description of Three of the Most Promising Molecules across All Datasets and Retrievals

| Molecule | Earth Abundance | Source (Earth) | Max Abundance Elsewhere | Source (Elsewhere) | References |
|---|---|---|---|---|---|
| DMS $(CH_3)_2S$ | $\lesssim$1 ppbv | Algae, marine organisms | $\approx$100 pptv | Cometary matter, ISM | (a) |
| Methacrylonitrile ($C_4H_5N$) | Unknown | Chemical synthesis, polymer production | $\approx$10 pptv | Interstellar molecular cloud | (b) |
| Allyl chloride ($C_3H_5Cl$) | Unknown | Chemical synthesis | Unknown | Unknown | (c) |

**Note.** This table summarizes their abundances and primary sources on Earth and elsewhere in the Universe (whether that location is a planet, a comet, or the ISM). Note that ppmv, ppbv, and pptv, mean parts per million, parts per billion, and parts per trillion by volume, respectively.
**References.** (a) E. L. Mungall et al. (2016), S.-B. Yan et al. (2023), P. Liss et al. (1993), T. Groene (1995), N. Hänni et al. (2024), and M. Sanz-Novo et al. (2025); (b) N. Grassie & E. Vance (1956), M. Y. Farooqui & M. M. Mumtaz (1991), and J. Cernicharo et al. (2022); and (c) A. R. Berger & H. H. Schaumburg (2005) and W. Wang et al. (2014).

result in the MIR data, finding a $\log_{10}$ volume mixing ratio of $-2.84^{+0.97}_{-1.29}$ with the VIRA retrievals of the MIRI JExoRES dataset, and $-2.91^{+1.03}_{-1.36}$ when using the JexoPipe data instead.

W26 employed photochemical modeling using VULCAN and Photochem and also a 1D radiative–convective–photochemical equilibrium model (their Extended Figure 3) to demonstrate that some hydrocarbons ($CH_4$, $C_2H_2$, $C_2H_4$, $C_2H_6$, $C_3H_4$, and $C_6H_6$) can be present in abundances greater than 1 ppmv between the 0.001 and 1 mbar pressure range, stating that the simulated atmosphere motivates the inclusion of the HITRAN hydrocarbons (I. E. Gordon et al. 2022) in their MIRI retrievals.

The W26 photochemical results, intended to show that hydrocarbons can be produced in temperate $H_2$-dominated atmospheres (particularly propyne at $\sim$10 ppmv), are however illustrative rather than quantitative matches to the retrieved abundances for K2-18 b. For instance, the predicted abundances for $H_2O$, CO, and $NH_3$ are factors of $\sim$110, $\sim$660, and $\sim$20 times higher, respectively, than the $2\sigma$ upper limits from the AURA retrievals in R. Hu et al. (2025), and similarly inconsistent with the results from other retrieval codes quoted in the same study. Additionally, the detection of $H_2S$ and $SO_2$ has not been reported in any K2-18 b transits, but the W26 photochemical models have such molecules at mixing ratios of $\approx 5 \times 10^{-3}$ and $\approx 10^{-4}$, respectively. These abundances might enable $H_2S$ and $SO_2$ to be detected, although it is important to state that the nondetection of a molecule does not imply its absence from the atmosphere. Photochemical modeling by Z. Huang et al. (2024) predicts propyne at mixing ratios up to $\sim 10^{-2}$. However, these models also result in abundances for both detected gases ($CH_4$ and $CO_2$) and nondetected gases (e.g., $H_2O$, $NH_3$, and CO), which are inconsistent with, respectively, their retrieved abundances and their upper limits (M23; R. Hu et al. 2025). Thus, it remains to be seen if the abundance of propyne inferred from the MIR observations could be explained by photochemistry on K2-18 b. More generally, the plausibility of any given species in the atmospheres of exoplanets should be considered in the context of the known chemical constraints and account for all the uncertainties present in the observations, retrievals, and photochemical models.

Another molecule of interest is cyclohexane, which is an industrial product on Earth used as a solvent or to make nylon and pesticides (E. A. Dada & L. Achenie 2012). Its emissions into Earth's atmosphere come from the petrochemical industry (Y. Liu et al. 2008) and vehicles (J. J. Schauer et al. 2002). It has been identified in the essences and oils of several plants (A. J. MacLeod & N. Gonzales de Troconis 1982; M. G. Gundidza & J. H. Zwaving 1993; A. J. Macleod et al. 1988). No predictions for its presence in planetary atmospheres at observable mixing ratios have been made, but it is hypothesized to be present in the ISM (S. Pilling et al. 2012).

Butane can reach up to abundances $\approx$10 ppbv in Earth's atmosphere due to it being a component of natural gas used as fuel. It is also emitted by plants (J. J. Schauer et al. 2001). It has been searched for in Titan's atmosphere; however, no confirmation of its presence has yet been made (B. L. Steffens et al. 2022). Results from Cassini's INMS indicate that butane is present in Saturn's atmosphere at mixing ratios of $\lesssim$5 ppmv (J. Serigano et al. 2022).

Overall, most of the molecules discussed above have not been found to have significant abiotic sources on Earth or beyond. In a few cases, some astrophysical sources are known to produce them in small quantities but their relevance to explain significant abundances in a planetary atmosphere is not clear, as discussed in Sections 2 and 6. These include methacrylonitrile, propyne, butane, and DMS. Therefore, future theoretical studies need to investigate potential biotic and abiotic mechanisms to assess the plausibility of these molecules on K2-18 b, if robustly confirmed with future observations.

## 6. Summary and Discussion

The JWST observations of the transmission spectrum of K2-18 b have opened a new avenue to characterize the atmospheres of temperate sub-Neptunes. In particular, the inference of DMS and/or DMDS in the atmosphere of K2-18 b (M23, M25) has opened the possibility of detecting potential biosignatures in habitable-zone exoplanets. However, any robust identification of a biosignature gas requires enough observations to achieve strong statistical evidence for it, as well as comprehensive theoretical works to assess the robustness of the inferences, including identifying potential false positives. In this work, we conduct a systematic and wide-ranging search for trace molecules in the atmosphere of K2-18 b, both to identify new potential species as well as to find viable alternatives to DMS and/or DMDS reported previously. We conduct this search using atmospheric retrievals over a large modeling space spanning contributions from 661 molecules. To ensure robustness of the results, we conduct atmospheric retrievals with three different data instances corresponding to two independent observations across the NIR and MIR, and validate them using three independent retrieval codes.

**Table 5**
Description of the Species Discussed in Section 5.3

| Molecule | Earth Abundance | Source (Earth) | Max Abundance Elsewhere | Source (elsewhere) | References |
|---|---|---|---|---|---|
| Propyne ($C_3H_4$) | $\lesssim$20 pptv | Laboratory, fuel | $\approx$4 ppmv | Atmospheric photochemistry, disk chemistry, ISM | (a) |
| Cyclohexane ($C_6H_{12}$) | Unknown | Industrial, plants | Unknown | Suggested to be in the ISM | (b) |
| Butane ($C_4H_{10}$) | $\lesssim$10 ppbv | Fuel, plants | $\lesssim$5 ppmv | Atmospheric chemistry | (c) |

**Note.** This table summarizes their abundances and primary sources on Earth and elsewhere in the Universe (whether that location is a planet, a comet, or the ISM). Note that ppmv, ppbv, and pptv, mean parts per million, parts per billion, and parts per trillion by volume, respectively.
**References**: (a) A. L. Steiner et al. (2008), C. A. Nixon et al. (2013), T. Fouchet et al. (2000), J. H. Waite et al. (2005), and L. E. Snyder & D. Buhl (1973); (b) A. J. MacLeod & N. Gonzales de Troconis (1982) and S. Pilling et al. (2012); and (c) J. J. Schauer et al. (2001, 2002), S. Rossabi & D. Helmig (2018), B. L. Steffens et al. (2022), and J. Serigano et al. (2022).

Our work represents a key advancement in the search for chemical species in temperate exoplanetary atmospheres with K2-18 b serving as a benchmark. The broad spectral range and high sensitivity of JWST has led to searches of increasing numbers of molecules in the atmosphere of K2-18 b. The molecular space spanned 11 species in M23, 20 in M25 and 92 (one by one) in W26, while considering a specific wavelength range and retrieval code each. The present work spans the full range of data available, and it uses a substantially enhanced set of 661 molecules, considered individually. As such, our results mark an important step toward comprehensive and agnostic searches for chemical signatures in exoplanetary atmospheres.

Across the 661 molecules considered, we find only one molecule, DMS, that reach Bayes factors compatible with moderate evidence ($\ln B \geqslant 2.0$) when all data and retrieval codes are considered, and when uncertainties in the estimation of Bayes factors are taken into account. We find that eight molecules may reach moderate evidence levels in both available MIRI datasets obtained using two different pipelines, and with all three retrieval codes used in this work. We tested whether any of these molecules also had evidence in the NIR (1–5 $\mu$m) transmission spectrum reported by M23. Of these, only one, DMS, reaches model preference values consistent with moderate evidence ($\ln B \geqslant 2.0$) with all three retrieval codes if no offsets are considered between NIRISS and NIRSpec; one more (methacrylonitrile) does so with `POSEIDON` and `VIRA`, but not with `pRT`. No individual species reached the moderate evidence or weak evidence threshold when allowing for an offset between the two instruments, although weak evidence is found, with `POSEIDON`, for a combination of DMS and methacrylonitrile.

Besides the molecules noted above, we find that several other molecules could explain at least some of the data considered. For example, propyne leads to significant model preferences with the MIRI data but not the NIR data. Second, we note that most of the retrievals explored in this work consider the contributions of 661 molecules individually, in addition to $CH_4$ and $CO_2$, which were inferred through the NIR observations, although not through the MIRI ones, due to the low prominence of their spectral features in the instrument's spectral range (see Figure 2). However, future studies could explore combinations of these molecules that could provide comparable or better fits to the data compared to the present results. We note that, following the standards in the field, we rely on Bayesian analysis to assess the quality of fits, as frequentist metrics (such as $\chi^2$) suffer from a number of flaws which make them unsuitable in the context of atmospheric retrievals and hypothesis testing (L. Welbanks et al. 2023).

Consideration of maximal models in this work has shown up to moderate evidence ($\ln B = 3.2$) for excess absorption beyond standard CNO species ($CH_4$, $CO_2$, $H_2O$, CO, $NH_3$, and HCN) across the considered spectral range. However, the contribution of the individual complex species which were revealed by the canonical models to be preferred remained degenerate. We highlight that it is also possible that some of the molecules explored may have strong features in only one of the two wavelength ranges, NIR or MIR, and hence may not be detectable in the other. Further observations could provide more stringent constraints on all these molecules, and lift degeneracies between them.

Our results have important implications for the possibility of DMS in the atmosphere of K2-18 b. Previous studies reported moderate evidence for DMS with a potential degeneracy with DMDS. The present study confirms that the previously reported evidence for DMS (M23, M25) is independent of the retrieval code used and persists across the datasets considered. Furthermore, of the promising molecules discussed above, DMS is the only one for which production mechanisms have been theorized which can explain its retrieved abundance on K2-18 b (N. Madhusudhan et al. 2021; S.-M. Tsai et al. 2024). A close second in terms of overall model preference, methacrylonitrile is also biogenic on Earth, but present in negligible amounts in the atmosphere. This molecule has not been identified in any other planet, and has no known significant abiotic pathways that can explain the retrieved abundances if present on K2-18 b. In addition, it is more complex than DMS and therefore harder to synthesize. If its presence is confirmed with future observations, theoretical studies would need to investigate its possible biotic or abiotic formation mechanisms on K2-18 b.

### 6.1. Toward Systematic Molecular Searches

In this work, we report an early protocol for systematic and agnostic searches of molecular species in exoplanetary atmospheres, following initial steps in M25 and W26. We considered nearly the full inventory of available cross sections in HITRAN (I. E. Gordon et al. 2022), and assessed whether the available data provided any support for each species considered individually. Future work in this direction could explore any possible evidence for combinations of species beyond those considered in current and previous works.

Following M25, our work demonstrates the effectiveness of using atmospheric retrievals and model preference values on a wide array of canonical models as a practical metric to restrict a very wide initial pool of species to a short list of likely candidates. In principle, an agnostic maximal model, including all considered species at once, could also be constructed, and

the nested model comparison approach as described in B. Benneke & S. Seager (2013) could be followed. However, at the present time it is computationally prohibitive to build an exhaustive maximal model. Any choice of maximal model would thus inevitably be somewhat arbitrary, unless supported by other theoretical and empirical considerations.

Nevertheless, further work on the canonical model approach we present should also explore in greater detail its statistical aspects. For example, two opposite effects remain unaddressed. First, our work, as an early exploratory search, considers hundreds of possible species to explain the signs of excess absorption in the spectra of K2-18 b, and arrives at a ranking based on the Bayesian preferences obtained across our workflow. While this allows for a more agnostic analysis, it also introduces the multiple comparisons problem, i.e., the fact that, when a large number of hypotheses is considered to explain a given dataset, it may be expected that some result in "statistically significant" results due to purely stochastic effects (e.g., Y. Benjamini & Y. Hochberg 1995; Y. Benjamini 2010). This is a greater concern in frequentist analyses, where the statistical significance of a result is directly determined by its $p$-value (e.g., R. L. Wasserstein & N. A. Lazar 2016). However, it may also be of concern in Bayesian comparisons, and hence require greater caution in the interpretation of the Bayes factors obtained for any given retrieval exploration of a dataset. Conversely, it is a general principle that the probability of independent events occurring jointly is always lower than the probability of each event individually. Thus, the fact that notable moderate preference is obtained for the same species on K2-18 b across three separate datasets corresponding to two independent observations at different wavelengths, with three different retrieval codes, makes it more likely that this result is due to a real signal, rather than random noise in the data. Future work should be carried out to accurately quantify these two effects, in order to arrive at a better interpretation of the quantitative results we present in this work.

### 6.2. The Importance of Assessing Physical Plausibility

An agnostic exploration carried out through retrievals must also be accompanied by considerations on the physical plausibility of results in the relevant context. For example, for any inferred species, potential production mechanisms—whether photochemical, thermochemical, geological, or even biological—should be assessed, while remaining open to the possibility of unknown mechanisms existing. Furthermore, the presence in detectable amounts of species with significant sinks—such as solubility for methacrylonitrile, or photochemistry for DMS (e.g., S.-M. Tsai et al. 2024)—may require constant re-generation mechanisms.

Due consideration should also be given to the plausibility of any inferred species being detectable at the thermodynamic conditions inferred for the atmosphere. For example, DMS, cyclohexane, and methacrylonitrile are liquids at room temperature and pressure on Earth (D. Lide 2007), although some of them readily vaporize under certain conditions. DMS has a lower boiling point and a higher vapor pressure when compared to methacrylonitrile, meaning that it is less likely to condense out in a temperate atmosphere. Observational constraints on the atmosphere's $P$–$T$ profile, together with theoretical studies on the phase these molecules may be expected to be found in at different thermodynamic conditions, may help in assessing the plausibility of their presence in the atmosphere of K2-18 b and of other temperate sub-Neptunes. It is however essential to be always aware of the possibility that unknown, exotic mechanisms may be at play in exoplanetary atmospheres, and thus caution should always be exercised when rejecting an empirically favored solution solely on the basis of present theoretical models.

### 6.3. Future Directions

Future work in this direction should involve both observational and theoretical efforts to increase the robustness of the findings and to assess their physical plausibility. More observations will be able to increase the statistical significance of the present inferences and break potential degeneracies between the different molecules. Theoretical work is needed on multiple fronts. Further exploration of promising combinations of molecules may provide better alternatives to the present molecular inferences and also provide additional insights into the atmospheric composition of K2-18 b. While we consider the MIRI and NIR datasets as separate, future work may consider joint retrievals on them. This has already been attempted in, e.g., R. Luque et al. (2025) and R. Hu et al. (2025). However, the lack of a robust prescription to account for the very different resolutions and signal-to-noise ratios of the MIRI and the NIR instruments has led to negligible differences in the retrieval results due to the MIRI data in such combined retrievals. Work is required to arrive at a well-motivated and robust prescription to account for this effect in atmospheric retrievals. At the same time, our work has highlighted the acute need for extensive molecular cross-section data, both for new molecules as well as for a wide range of conditions, including different pressures, temperatures, and $H_2$ broadening for available cross sections. Finally, theoretical work is also needed to assess the physical plausibility of any inferred molecule given the astrophysical context of the exoplanet concerned.

Our work highlights the requirement for a comprehensive assessment of all available evidence linked to the physical plausibility of specific molecules being present in a planetary atmosphere, including potential biosignatures. At the same time, it demonstrates the capability of atmospheric retrievals, when used with the appropriate robustness checks, to rise to the challenge provided by the JWST datasets, and dramatically restrict the number of species whose presence may be inferred from the data, even when operating on an agnostic basis. The onset of JWST transmission observations of K2-18 b across the NIR and MIR wavelengths has enabled an exciting new phase of discovery in the temperate sub-Neptune regime. Further confirmation of DMS, or of other molecules considered herein, could have wide-ranging implications, from potential biosignatures to exotic abiotic chemistry.

## Acknowledgments

N.M. and L.P.C. acknowledge support from the Science & Technologies Facilities Council (STFC) toward the PhD studies of L.P.C. (UKRI grant No. 2886925). N.M., S.C., and G.J.C. acknowledge support from the UK Research and Innovation (UKRI) Frontier grant (grant No. EP/X025179/1; PI: N. Madhusudhan). N.M. and M.B. acknowledge support from the UK Research and Innovation (UKRI) Frontier grant

(grant No. EP/X025179/1; PI: N. Madhusudhan) toward the PhD studies of M.B., and N.M. and G.J.C. acknowledge support from the Leverhulme Centre for Life in the Universe. The authors would like to thank Måns Holmberg and Julianne I. Moses for helpful discussions.

## Appendix A
## Model and Retrieval Specifications

In Tables 6 and 7, we report our retrieval and model settings, as well as the prior distributions and descriptions for the free parameters included in our retrievals.

## Appendix B
## Results from MIRI Retrievals

Table 8 includes the Bayes factors obtained from MIRI canonical retrievals with POSEIDON for all species resulting in $\ln B \geqslant 1.15$ when using at least one of JexoPipe or JExoRES dataset. We choose $\ln B \geqslant 1.15$ as this corresponds to the threshold for "substantial" evidence in the H. Jeffreys (1948) original scale, and is well within the "weak evidence" and "positive evidence" categories in, respectively, R. Trotta (2008) and R. E. Kass & A. E. Raftery (1995). After the table, we list all remaining species, for which we ran canonical model retrievals on both MIRI datasets, but which resulted in $\ln B < 1.15$ in both pipelines.

**Table 6**
Values of the Retrieval Settings and Model Specifications Employed across This Study

| Parameter | POSEIDON | VIRA | pRT | Description |
|---|---|---|---|---|
| $P$ grid | $10 - 10^{-6}$ bar, 100 layers | $10 - 10^{-7}$ bar, 100 layers | $10 - 10^{-6}$ bar, 100 layers | Pressure grid for the atmosphere |
| $\lambda$ array (MIR) | 6000 points, 4.8 − 12.0 $\mu$m, equal spacing in $\lambda$ | 6000 points, 4.8 − 12.0 $\mu$m, equal spacing in $\lambda$ | Constant $R = 1000$, 4.8 − 12.0 $\mu$m | Wavelength array for MIRI retrievals |
| $\lambda$ array (NIR) | 25, 000 points, 0.5 − 5.2 $\mu$m, equal spacing in $\lambda$ | 22, 000 points, 0.45 − 5.5 $\mu$m, equal spacing in $\lambda$ | Constant $R = 1000$, 0.5 − 5.2$\mu$m | Wavelength array for NIR retrievals |
| $R$ (10 $\mu$m) | $R(10\mu\text{m}) = 8332$ $170 \times R_{\text{data}}(10\ \mu\text{m})$ | $R(10\mu\text{m}) = 8332$ $170 \times R_{\text{data}}(10\ \mu\text{m})$ | Correlated-K | Resolution at 10 $\mu$m, absolute and relative |
| $R$ (3 $\mu$m) | $R(3\mu\text{m}) = 15957$ $3.6 \times R_{\text{data}}(3\ \mu\text{m})$ | $R(3\mu\text{m}) = 13069$ $2.9 \times R_{\text{data}}(3\ \mu\text{m})$ | Correlated-K | Resolution at 3 $\mu$m, absolute and relative |
| Live points | 2000 | 2000 for MIRI 1000 for NIR | 500 | Number of live points for MultiNest |
| Sampling efficiency | 0.3 | 0.3 | 0.3 | Sampling efficiency for MultiNest |

**Note.** In VIRA, supersampling is used to sample the cross sections at a higher resolution (when available) than the grid resolution in the forward model. In pRT, correlated-K opacities are used. We also use supersampling in the NIR with POSEIDON; we considered the same in the MIR as well but saw no significant effect. Depending on the species, the native resolution of opacities before supersampling is up to $R \sim 3.3 \times 10^5$ at 3 $\mu$m and $R \sim 10^5$ at 10 $\mu$m.

**Table 7**
Form and Range of the Bayesian Prior Distributions for the Free Parameters in all of the Atmospheric Retrievals Carried out in This Work

| Parameter | Priors | Description |
|---|---|---|
| log(X) | $\mathcal{U}(-12, -0.3)$ | Volume mixing ratio of each molecule (VIRA and POSEIDON) |
| $\log(X_{\text{mass}})$ | $\mathcal{U}(-11, -0.1)$ | Mass mixing ratio of each molecule (pRT) |
| $T_0$/K | $\mathcal{U}(100, 500)$ | Temperature at the top of the atmosphere |
| $\alpha_1/\text{K}^{-\frac{1}{2}}$ | $\mathcal{U}(0.02, 2.00)$ | $P$–$T$ profile curvature |
| $\alpha_2/\text{K}^{-\frac{1}{2}}$ | $\mathcal{U}(0.02, 2.00)$ | $P$–$T$ profile curvature |
| $\log(P_1/\text{bar})$ | $\mathcal{U}(-6, 0)$ | $P$–$T$ profile region limit |
| $\log(P_2/\text{bar})$ | $\mathcal{U}(-6, 0)$ | $P$–$T$ profile region limit |
| $\log(P_3/\text{bar})$ | $\mathcal{U}(-2, 0)$ | $P$–$T$ profile region limit |
| $\log(P_{\text{ref}}/\text{bar})$ | $\mathcal{U}(-6, 0)$ | Reference pressure, at $R_p = 2.61\ R_\oplus$ |
| $\log(a)$ | $\mathcal{U}(-4, 10)$ | Rayleigh enhancement factor |
| $\log(\gamma)$ | $\mathcal{U}(-20, 2)$ | Scattering slope ($\sigma \sim \lambda^\gamma$) |
| $\log(P_c/\text{bar})$ | $\mathcal{U}(-6, 0)$ | Cloud-top pressure |
| $\phi$ | $\mathcal{U}(0, 1)$ | Cloud/haze coverage factor |
| $\delta$/ppm | $\mathcal{U}(-100, 100)$ | Offset between NIRISS and NIRSpec detectors, when applicable |

**Table 8**
Comparison of the Natural Log Bayes Factors and Significance ($\ln B$ and $\sigma$) for Molecules Retrieved Using POSEIDON from JWST MIRI Observations, Which Result in $\ln B \geqslant 1.15$ for at Least one of the JExoRES and JexoPipe Reductions

| Molecule | JExoRES | | JexoPipe | | Cross-section Metadata | | |
|---|---|---|---|---|---|---|---|
| | $\ln B$ | $\sigma$ | $\ln B$ | $\sigma$ | $P$ (bar) | $T$ (K) | Range ($\mu$m) |
| Chloroethane | 3.06 | 2.97 | 3.95 | 3.28 | 1.01 | 298.10 | 1.54–16.95 |
| Cyclohexane | 2.53 | 2.77 | 2.98 | 2.94 | 1.01 | 298.10 | 1.54–17.54 |
| Dichloromethane | 2.55 | 2.78 | 2.79 | 2.87 | 1.01 | 298.10 | 1.54–16.67 |
| Propyne | 2.56 | 2.78 | 2.74 | 2.85 | 1.01 | 298.10 | 1.49–17.86 |
| Bromoethane | 2.64 | 2.81 | 2.04 | 2.56 | 1.01 | 298.10 | 1.54–18.87 |
| Methacrylonitrile | 2.56 | 2.78 | 2.37 | 2.70 | 1.01 | 298.10 | 1.54–19.23 |
| 2-butene (cis and trans) | 2.51 | 2.76 | 0.84 | 1.92 | 1.01 | 298.10 | 1.54–18.18 |
| Tetramethylsilane | 1.59 | 2.35 | 2.51 | 2.76 | 1.01 | 298.10 | 1.35–18.18 |
| DMS | 2.22 | 2.64 | 2.51 | 2.76 | 1.01 | 298.10 | 1.54–16.67 |
| Butane | 2.45 | 2.73 | 2.14 | 2.60 | 1.01 | 298.10 | 1.54–16.67 |
| Methacryloyl chloride | 2.43 | 2.73 | 1.27 | 2.18 | 1.01 | 298.10 | 1.54–18.87 |
| Methacrolein | 2.42 | 2.72 | 1.25 | 2.17 | 1.01 | 298.10 | 1.54–16.67 |
| Dimethyl carbonate | 1.45 | 2.28 | 2.39 | 2.71 | 1.01 | 298.10 | 1.54–17.39 |
| Cyclopentane | 2.38 | 2.70 | 2.16 | 2.61 | 1.01 | 298.10 | 1.54–19.61 |
| Dichloromethylphosphine | 1.02 | 2.04 | 2.32 | 2.68 | 1.01 | 298.10 | 1.54–19.23 |
| DMDS | 2.30 | 2.67 | 1.91 | 2.50 | 1.01 | 298.10 | 1.54–16.67 |
| 1-chloropentane | 1.22 | 2.15 | 2.17 | 2.62 | 1.01 | 298.10 | 1.54–16.95 |
| Allyl chloride | 2.14 | 2.60 | 2.05 | 2.56 | 1.01 | 298.10 | 1.54–19.05 |
| Ethanethiol | 1.36 | 2.23 | 2.08 | 2.58 | 1.01 | 298.10 | 1.54–17.09 |
| Trans-2-pentene | 2.02 | 2.55 | 1.05 | 2.05 | 1.01 | 298.10 | 1.54–18.18 |
| Diethyl sulfide | 1.77 | 2.44 | 1.96 | 2.52 | 1.01 | 298.10 | 1.54–16.67 |
| Boron trichloride | 1.93 | 2.51 | 0.86 | 1.93 | 1.01 | 298.10 | 1.54–16.67 |
| Tetradecane | 1.55 | 2.33 | 1.92 | 2.50 | 1.01 | 298.10 | 1.54–17.24 |
| Iodomethane | 1.88 | 2.49 | 1.59 | 2.35 | 1.01 | 298.10 | 1.45–20.00 |
| 1-chlorobutane | 1.00 | 2.02 | 1.68 | 2.39 | 1.01 | 298.10 | 1.54–18.52 |
| Tungsten hexafluoride | 1.52 | 2.31 | 0.68 | 1.81 | 1.01 | 298.10 | 1.54–16.67 |
| Isobutylene | 1.41 | 2.25 | 1.27 | 2.18 | 1.01 | 298.10 | 1.54–16.67 |
| Chlorine nitrate | 0.21 | 1.39 | 1.39 | 2.24 | 0.10 | 297.40 | 7.58–7.94 |
| Iodoethane | 1.33 | 2.21 | 0.21 | 1.39 | 1.01 | 298.10 | 1.54–16.67 |
| 2-methylbutane | 1.01 | 2.03 | 1.32 | 2.21 | 1.01 | 298.10 | 1.54–16.67 |
| Calcium oxide | 1.21 | 2.15 | 1.19 | 2.13 | … | … | … |
| Neopentane | 0.61 | 1.76 | 1.19 | 2.14 | 0.14 | 293.80 | 6.45–8.13 |
| Ethane | 1.19 | 2.13 | 0.65 | 1.79 | … | … | … |
| 1,1-dichloroethane | 0.74 | 1.85 | 1.19 | 2.13 | 1.01 | 298.10 | 1.54–17.86 |
| 2,2-dimethylbutane | 1.15 | 2.12 | 0.59 | 1.74 | 1.01 | 298.10 | 1.54–16.67 |
| Pentane | 0.89 | 1.96 | 1.15 | 2.11 | 1.01 | 298.10 | 1.54–17.54 |

**Note.** The Bayes factors are for the canonical model with the relevant molecule included, versus an identical baseline model only including $CH_4$ and $CO_2$, as discussed in Section 3. The Bayesian evidence of the reference model against which the Bayes factors are reported is $\ln(Z) = 212.82$ when using the JExoRES data and $\ln(Z) = 208.18$ with the JexoPipe data. Associated cross-section metadata are also included for species not originally present in the POSEIDON database.

### *B.1. Remaining Species*

Bromine nitrate; boron trifluoride; 3-methylpentane; propylene; cyclopropane; 1-butyne; cycloheptane; methyltrichlorosilane; 1-pentene; acetylene; hydrogen cyanide; diethyl sulfate; 1,2-epoxybutane; 2-methyl-1-pentene; 2-vinylpyridine; cis-2-pentene; sulfuryl fluoride; propargyl chloride; hexane; cis-4-methyl-2-pentene; ethylene; benzene; dimethyl sulfate; 3-methyl-1-butene; propylene oxide; 2-methyl-1-butene; 1-heptene; cyanogen chloride; chloromethane; hexanal; 3-methylhexane; 1-hexene; 1-butene; isophorone; heptane; allyl bromide; 1-octene; acrylonitrile; 1-chloro-2-methylpropane; cyclodecane; 1,3-dichloropropane; water; decane; butyraldehyde; phosphorus monosulfide (PS); dimethyl sulfoxide; methylium; 1,2-dichloroethane; 1-propan ethiol; undecane; octane; pentyl nitrate; nonane; styrene; 1-nonene; N,n-diethylformamide; 1-decene; 1,2,3-trimethylbenzene; 1,1,1-trifluoroethane; isoprene; sec-butylbenzene; 1-undecene; propionitrile; propane; limonene oxide; 4-methyl-1-pentene; 4-ethyltoluene; (-)-beta-pinene; 1,3-butadiene; di-isobutylene; isobutyraldehyde; 3-carene; magnesium monohydride; cis-1,2-dichloroethylene; HFC-272ca; tridecane; valeraldehyde; 2-methylstyrene; thiophene; scandium monohydride; 2,2,4-trimethylpentane; 2,3-dimethylbutane; vinyl chloride; 2-methy lpentane; 3-methylbutanal; lithium hydride; 1,2,3,5-tetramethylbenzene; 3,4-dichloro-1-butene; 2-methyl-2-butene; methyl vinyl ketone; vanadium(ii) oxide; 1,2,3,4-tetramethylbenzene; pentadecane; tert-butylbenzene; epichlorohydrin; 2,5-dimethylfuran; geraniol; but-2-ynenitrile; allyl isothiocyanate; 2-methylaziridine; 2-methyl-2-pentene; 2,4,4-trimethyl-2-pentene; ethylbenzene; 1,2-dichloropropane; propyl acetate; isobutyl acetate; limonene; isobutane; titanium monoxide; 4-methylpyridine; amyl acetate; mesitylene; methyl acrylate; 1,2,3-trichloropropane; cumene; hexyl acetate; 1,1,1,2-tetrachloroethane; 1,4-dichlorobenzene; thiirane; O-xylene; aluminum monohydride; 1-ethyl-2-methylbenzene; glycolaldehyde; chlorocyclohexane; propionaldehyde; diketene; butyl acetate; carbon tetrafluoride; P-xylene; cyclooctane; carbon

monosulfide; D-limonene; silicon monohydride; zirconium oxide (ZrO); imidogen; aluminum monoxide; germane; 1,1,1,3,3,3-hexafluoropropane; cycloheptene; 2-methylpyridine; bromobenzene; titanium; methylglyoxal; lithium; propargyl alcohol; hydrogen sulfide; hexafluorobenzene; cyanoacetylene; toluene; propylbenzene; sodium; N,n-dimethylformamide; hydrofluoric acid; 2,4-dimethylpentane; isobutyronitrile; atomic oxygen; scandium; ammonia; cesium; barium cation; (Z)-HFC-1234ze; butyl isocyanate; methyl acetate; trans-1,3-dichloropropene; myrcene; barium; OH; styrene oxide; benzyl alcohol; nitric oxide; OH+; ethyl acrylate; hydrochloric acid; chromium; 4-chlorotoluene; carbon monoxide; magnesium; ethynid-2-yl; furfural; sodium hydroxide; iron; methanesulfonyl chloride; nickel carbonyl; magnesium cation; iron cation; acetonitrile; cyclohexanethiol; 2-carene; (-)-alpha-pinene; calcium; MgO; H3+; aluminum; methylidyne radical; vanadium; iron monohydride; calcium cation; 4-vinylcyclohexene; titanium cation; lanthanum monoxide; hydrosulfide (SH); rubidium; isoamyl acetate; potassium; chloroform; nanganese; carbon disulfide; potassium chloride; chromium(I) hydride; vanadium cation; chloroacetone; methanethiol; titanium monohydride; 1-fluorohexane; 1,2,3,4-tetrahydronaphthalene; nickel; methyl isocyanate; M-xylene; propylene sulfide; phosphorous nitride (PN); beryllium monohydride; tetrahydrothiophene; hydroxyacetone; 2-propanethiol; trichloroacetyl chloride; hexadecane; sulfur hexafluoride; allene; nitrous oxide; isobutyl mercaptan; butyl acrylate; glyoxal; thioformaldehyde; 5-methyl-2-hexanone; cyclohexene; allylamine; 3-methylpyridine; acryloyl chloride; 3-ethyltoluene; benzonitrile; 1,1,1-trichloroethane; cyclopentene; silicon monoxide; carbonyl sulfide; methyl isothiocyanate; ethyl acetate; 2-chloroethanol; 2-nonanone; 4-methyl-2-pentanone; sodium monoxide radical (NaO); 5-nonanol; naphthalene; bromochloromethane; 3-pentanone; titanium tetrachloride; 1-penten-3-ol; chlorosulfonyl isocyanate; trimethylamine; tert-amylamine; vinyl bromide; octafluorocyclobutane; 1-undecanol; potassium hydroxide; butylamine; 2-methyl-1-propanol; nitrosyl chloride; calcium monohydride; 1-hexanol; acetaldehyde; 2-hexanone; 1-nonanol; 1-butanol; 2-pentanone; 4-penten-1-ol; allyl fluoride; 2-mercaptoethanol; 4-methyl-1-pentanol; quinoline; 2-chlorotoluene; allyl alcohol; methanol; methyl benzoate; 1,1,2-trichloroethane; fluoroacetone; 3-methyl-2-pentanone; trichloroethylene; sodium hydride; 1-pentanol; menthol; tetrafluorosilane; perfluoroisobutylene; 2-chloropropane; diacetone alcohol; 2-butanone; ethanol; sulfur monoxide; furfuryl alcohol; pentane-1,5-diamine; 3,3-dimethyl-2-pentanol; boron tribromide; 2-bromopropane; isoamyl alcohol; methyl methacrylate; 2-butanol; cyclohexanone; phosphorus monoxide; 1-heptanol; acrolein; 1-propanol; 2-ethylhexan-1-ol; tert-butyl acetate; 2,3-butanedione; 1,1-dimethylhydrazine; nitrogen trifluoride; isocyanic acid; triethylamine; 3-pentanol; allyl iodide; acetic acid; 1,1,2,2-tetrachloroethane; pyridine; silane; hexafluoroacetone; di-isopropylamine; arsine; 2-pentanol; 3-chlorotoluene; ozone; flurothyl; peroxyacetyl nitrate; tetrachloroethylene; 2-hexanol; ethylamine; crotonaldehyde; trans-2-butene; (e)-1,2,3,3,3-pentafluoroprop-1-ene; benzaldehyde; diethylamine; thiophosphoryl chloride; 2-pentylfuran; neopentyl alcohol; piperidine; 1,2-dibromo-3-chloropropane; dichlorosilane; ethyl benzoate; phosphorus oxychloride; 2,6-diethylaniline; 3-chloro-1,1,1-trifluoropropane; methylamine; hexamethylphosphoramide; 1,1,1,2,3,3,3-heptafluoropropane; methylhydrazine; fluoroethane; 2-iodopropane; 1,2-dichloroethylene; 3-methyl-2-butanone; dimethylamine; hydrazine; tert-butanol; sulfuryl chloride; 1,1,1,3,3-pentafluorobutane; perchloromethyl mercaptan; 3-methylfuran; nenzyl bromide; methyl pivalate; ethylene glycol; isopropylamine; 2-methylfuran; trifluoroacetyl chloride; isopropyl acetate; $NO_2$; HFE-263m1; sec-amylamine; cis-1,3-dichloropropene; cis-2-butene; phosphine; bromoform; trifluoroacetaldehyde; 1,1,1-trichlorotrifluoroethane; ethylenediamine; 1,2-difluoroethane; isopropyl alcohol; 1,3-dichlorobenzene; propylene glycol; 1,2-dichlorobenzene; methyl acetoacetate; 2-methyl-2-propanethiol; ethyl nitrite; 1-nitropropane; fluoromethane; O-toluidine; hexafluoropropene; nitroethane; di-iodomethane; 1,2-dibromoethane; 2,3-dichloro-1-propene; cyclohexanol; 2-methoxy-4-nitrophenol; nitrous acid; pentacarbonyliron; 1,1,1,2,2-pentafluoro-2-(trifluoromethoxy)ethane; sevoflurane; benzenethiol; nicotine; 1,1-difluoroethane; nitromethane; 2,2,2-trifluoroethyl methyl ether; acetyl chloride; trans-1,2-dichloroethylene; 1,1,1,2-tetrafluoroethane; furan; morpholine; 4-methylvaleric acid; perfluoropropane; texanol; 2-chloro-1,1,1-trifluoroethane; 2-ethoxyethyl acetate; acetone cyanohydrin; 3,3,3-trifluoropropanal; ethyl butyrate; methyl nitrite; methyl salicylate; eucalyptol; 3-methoxyperfluoro(2-methylpentane); bromodichloromethane; aniline; di-isopropyl ether; thionyl fluoride; 2-nitropropane; sulfur dioxide; trichloromethanol; methyl hexanoate; 3,3,3-trifluoropropene; 2-fluoroethanol; trifluoromethyl trifluorovinyl ether; 1,1,1,3,3,3-hexafluoro-2-propanol; 2,3-dimethylfuran; chlorobenzene; butyric acid; 2,3,3,3-tetrafluoro-2-(trifluoromethyl)propanenitrile; oxirane; dimethylcarbamoyl chloride; dipropyl ether; N,n-diethylaniline; 1,1,1,2,2-pentafluoropropane; trifluoromethyl perfluoropropyl ether; methyl propionate; 3,3,3-trifluoro-1-propanol; 4-methoxyphenol; methyl butyrate; vinyl acetate; tert-butyl ethyl ether; dichlorofluoromethane; 2-methoxy-5-nitrophenol; 1,2-dibromoethylene; dibromomethane; 1,2-dichlorofluoroethane; tetrahydrofuran; tert-butyl methyl ether; methyl 2-methyl butyrate; dichloromethanol; nonenedioic acid; perfluoro-2-methyl-3-pentanone; octanoic acid; perfluoroisohexane; chloromethyl ethyl ether; methyl vinyl ether; chlorodibromomethane; 1-methoxybutane; chlorotrifluoromethane; halothane; sulfur; pentafluoro(trifluoromethyl)-; hexanoic acid; 2-chloroethyl ethyl ether; benzoyl chloride; chloropentafluoroethane; dodecafluoropentane; tert-amyl methyl ether; guaiacol; 1,1-dichloro-1-fluoroethane; 1,2-dichloro-1,1-difluoroethane; Ppg-2 methyl ether; hexachlorocyclopentadiene; acrylic acid; nitrobenzene; 1,1,1,3,3-pentafluoropropane; methyl isobutyrate; 2-butoxyethanol; methyl nonafluoro-n-butyl ether; dinitrogen pentaoxide; 1,4-dioxane; trichlorofluoroethylene; 2-methoxyethanol; vinyl fluoride; hexafluoroisobutylene; trichlorofluoromethane; ethyl vinyl ether; trifluoronitrosomethane; 1,1,1,2-tetrafluoro-2-(trifluoromethoxy) ethane; allyl trifluoroacetate; (*Z*)-perfluorodecalin; HFE-245fa2; hexachloro-1,3-butadiene; M-cresol; methyl nonafluorobutyl ether; allyl 1,1,2,2-tetrafluoroethyl ether; chlorofluoromethane; chloromethyl methyl ether; chloromethanol; hexafluoroisopropyl methyl ether; 1,2-dichloro-1,2-difluoroethane; 1,1-dichlorotetrafluoroethane; valeric acid; 2,6-dimethoxyphenol; perflubutane; (E)-HCFO-1233zd; 1,2-dichloro-1,1,3,3,3-pentafluoropropane; 1,1,1-trifluoroacetone; chloropicrin; 1,1,2,2-tetrafluoro-3-methoxypropane; chlorotrifluoroethylene; isobutyric acid; fluorobenzene; 1-(ethoxy)nonafluorobutane; ethyl formate; propionic acid; 1h,1h,2h,2h-perfluoroheptan-1-ol; 2,2,3,3-tetrafluoro-1-propanol; 3,3,4,4,5,5,6,6,7,7,8,8,9,9,9-pentadecafluorononan-1-ol; 3-methoxyphenol; methyl formate; HFE-356mec3; 1,1-dihydroperfluoropropanol; ethyl chloroformate; 2,2,3,4,4,4-hexafluoro-1-butanol; tetrafluoroethylene; vinylidene chloride; CFC-112; 1,1,2,3,3,4,4,4-octafluorobut-1-ene; HG-10; HFE-7500; HFE-125; HFC-32; methoxyethane; HCFC-121; 1,1-dibromotetrafluoroethane; 1,1-dichloro-1,2-difluoroethane; thiophosgene; 2,4-di-

isocyanato-1-methylbenzene; chlorodifluoromethane; bis(2-chloroethyl) ether; dimethyl ether; 3,3,4,4,5,5,6,6,6-nonafluoro-1-hexene; 1,1,1,2,2,3-hexafluoropropane; 1,3-dioxolane; bromodifluoromethane; 2,2-dichloro-1,1,1-trifluoroethane; phenol; diethyl ether; dibromodifluoromethane; ethyl 1,1,2,3,3,3-hexafluoropropyl ether; hexafluoroethane; HFE-365mcf3; 2,2,2-trifluoroethanol; 1,1-difluorotetrachloroethane; heptafluorobutyraldehyde; 1,2-dimethoxy-1,1,2,2-tetrafluoroethane; dichlorodifluoromethane; HFC-43-10mee; 1,1,2-trifluoroethane; 2,3,3,3-tetrafluoropropene; 1,2-dimethoxyethane; nonafluoropentanal; heptafluoropropane; 2,2-difluoroethan-1-ol; 2-methyl-1,3-dioxolane; perfluoroheptane; propylene carbonate; methyl chloroformate; 1,1-dichloro-2,2-difluoroethane; 1,1,1,2,3,3-hexafluoropropane; 3,3,4,4,5,5,6,6,7,7,8,8,9,9,10,10,11,11,11-nonadecafluoroundecan-1-ol; (*E*)-perfluorodecalin; trifluoromethyl methyl ether; isoflurane; trifluoroacetic anhydride; pentafluoroethane; paraldehyde; dimethoxymethane; trifluoromethane; 2-chloro-1,1,1,2-tetrafluoroethane; hexafluoro-1,3-butadiene; 2,2,3,3,4,4,4-heptafluoro-1-butanol; (z)-1,2,3,3,3-pentafluoropropene; dichlorotetrafluoroethane; ethyl trifluoroacetate; diborane; 2,2,3,3,3-pentafluoropropanal; 1,1,2-trichlorotrifluoroethane; HG-02; 3,3,4,4,4-pentafluorobut-1-ene; 1-chloro-1,1-difluoroethane; enflurane; perfluorotributylamine; 1,2-dichloro-1,1,2-trifluoroethane; trifluoroacetic acid; 1h-perfluorohexane; 1,1,1,2,2,3,3,4,4-nonafluorobutane; perfluorohexane; acetic anhydride; desflurane; 3,3-dichloro-1,1,1,2,2-pentafluoropropane; 1-chloro-1,1,2,2-tetrafluoroethane; perfluoropolymethylisopropyl ether; propane; 1,1,1,2,2,3,3-heptafluoro-3-methoxy-; Perfluoro-2-methyl-2-pentene; HG-11; HFE-347pcf2; HFE-338mec3; vinyl trifluoroacetate; heptafluoropropyl 1,2,2,2-tetrafluoroethyl ether; 1h,1h,2h-perfluoro-1-decene; perfluorooctane; 1,3-dichloro-1,1,2,2,3-pentafluoropropane; (perfluorohexyl)ethylene; bromotrifluoromethane; 1,1,2,2-tetrafluoroethane; HG-03; bromochlorodifluoromethane; 1,1,2,2,3-pentafluoropropane; decamethylcyclopentasiloxane; and HG-01.

## ORCID iDs

Lorenzo Pica-Ciamarra https://orcid.org/0009-0008-9026-5534
Nikku Madhusudhan https://orcid.org/0000-0002-4869-000X
Gregory J. Cooke https://orcid.org/0000-0001-6067-0979
Savvas Constantinou https://orcid.org/0000-0001-6839-4569
Martin Binet https://orcid.org/0009-0003-4155-0500

## References

Ahrer, E.-M., Radica, M., Piaulet-Ghorayeb, C., et al. 2025, ApJL, 985, L10
Amrhein, V., Korner-Nievergelt, F., & Roth, T. 2017, PeerJ, 5, e3544
Andron, I., Gratier, P., Majumdar, L., et al. 2018, MNRAS, 481, 5651
Arabhavi, A. M., Kamp, I., Henning, T., et al. 2024, Sci, 384, 1086
Barshay, S. S., & Lewis, J. S. 1978, Icar, 33, 593
Bates, K. H., Jacob, D. J., Wang, S., et al. 2021, JGRD, 126, e2020JD033439
Beatty, T. G., Welbanks, L., Schlawin, E., et al. 2024, ApJL, 970, L10
Bello-Arufe, A., Hu, R., Zilinskas, M., et al. 2025, arXiv, arXiv:2511.15835
Belloche, A., Müller, H. S. P., Menten, K. M., Schilke, P., & Comito, C. 2013, A&A, 559, A47
Benjamini, Y. 2010, Journal of the Royal Statistical Society: Series B (Statistical Methodology), 72, 405
Benjamini, Y., & Hochberg, Y. 1995, Journal of the Royal Statistical Society: Series B (Methodological), 57, 289
Benneke, B., Roy, P.-A., Coulombe, L.-P., et al. 2024, arXiv, arXiv:2403.03325
Benneke, B., & Seager, S. 2013, ApJ, 778, 153
Benneke, B., Wong, I., Piaulet, C., et al. 2019, ApJL, 887, L14
Berger, A. R., & Schaumburg, H. H. 2005, Peripheral Neuropathy (Elsevier Inc.), 2505
Birkmann, S. M., Ferruit, P., Alves de Oliveira, C., et al. 2014, SPIE, 9143, 914308
Bouwman, J., Kendrew, S., Greene, T. P., et al. 2023, PASP, 135, 038002
Buchner, J., Georgakakis, A., Nandra, K., et al. 2014, A&A, 564, A125
Burgdorf, M., Orton, G., van Cleve, J., Meadows, V., & Houck, J. 2006, Icar, 184, 634
Carrión, O., Curson, A. R., Kumaresan, D., et al. 2015, NatCo, 6, 6579
Catling, D. C., Krissansen-Totton, J., Kiang, N. Y., et al. 2018, AsBio, 18, 709
Cernicharo, J., Fuentetaja, R., Cabezas, C., et al. 2022, A&A, 663, L5
Cloutier, R., Astudillo-Defru, N., Doyon, R., et al. 2019, A&A, 621, A49
Constantinou, S., & Madhusudhan, N. 2024, MNRAS, 530, 3252
Cooke, G. J., & Madhusudhan, N. 2024, ApJ, 977, 209
Courtin, R., Gautier, D., Marten, A., Bézard, B., & Hanel, R. 1984, ApJ, 287, 899
Dada, E. A., & Achenie, L. 2012, Computer Aided Chemical Engineering, 31 (Elsevier), 240
de Graauw, T., Feuchtgruber, H., Bezard, B., et al. 1997, A&A, 321, L13
Dittmann, A. 2024, OJAp, 7, 79
Domagal-Goldman, S. D., Meadows, V. S., Claire, M. W., & Kasting, J. F. 2011, AsBio, 11, 419
Doyon, R., Hutchings, J. B., Beaulieu, M., et al. 2012, SPIE, 8442, 84422R
Efstathiou, G. 2008, MNRAS, 388, 1314
Farooqui, M. Y., & Mumtaz, M. M. 1991, Toxgy, 65, 239
Fayolle, E. C., Öberg, K. I., Jørgensen, J. K., et al. 2017, NatAs, 1, 703
Felix, L., Kitzmann, D., Demory, B.-O., & Mordasini, C. 2025, A&A, 701, A296
Feroz, F., Hobson, M. P., & Bridges, M. 2009, MNRAS, 398, 1601
Ferruit, P., Bagnasco, G., Barho, R., et al. 2012, SPIE, 8442, 84422O
Fisher, R. A. 1934, Statistical Methods For Research Workers, http://archive.org/details/in.ernet.dli.2015.205971
Fouchet, T., Lellouch, E., Bézard, B., et al. 2000, A&A, 355, L13
Fulton, B. J., & Petigura, E. A. 2018, AJ, 156, 264
Gardner, J. P., Mather, J. C., Clampin, M., et al. 2006, SSRv, 123, 485
Gordon, I. E., Rothman, L. S., Hargreaves, R. J., et al. 2022, JQSRT, 277, 107949
Grant, D., Lewis, N. K., Wakeford, H. R., et al. 2023, ApJL, 956, L32
Grassie, N., & Vance, E. 1956, TrFS, 52, 727
Groene, T. 1995, JMS, 6, 191
Guélin, M., & Cernicharo, J. 2022, FrASS, 9, 787567
Gundidza, M. G., & Zwaving, J. H. 1993, JEOR, 5, 341
Hänni, N., Altwegg, K., Combi, M., et al. 2024, ApJ, 976, 74
Holmberg, M., & Madhusudhan, N. 2024, A&A, 683, L2
Hu, R., Bello-Arufe, A., Tokadjian, A., et al. 2025, arXiv, arXiv:2507.12622
Huang, J., Seager, S., Petkowski, J. J., Ranjan, S., & Zhan, Z. 2022, AsBio, 22, 171
Huang, Z., Yu, X., Tsai, S.-M., et al. 2024, ApJ, 975, 146
Hänni, N., Altwegg, K., Baklouti, D., et al. 2025, A&A, 699, A135
Jeffreys, H. 1948, Theory of Probability (2nd ed.; Clarendon)
Kass, R. E., & Raftery, A. E. 1995, JASA, 90, 773
Kendrew, S., Scheithauer, S., Bouchet, P., et al. 2015, PASP, 127, 623
Khan, M. A. H., Cooke, M. C., Utembe, S. R., et al. 2014, AtmEn, 99, 77
Kim, M.-S., Kim, J. H., Park, H.-S., et al. 2006, KJCE, 23, 919
Le Roy, L., Altwegg, K., Balsiger, H., et al. 2015, A&A, 583, A1
Ledyard, K. M., & Dacey, J. W. 1994, MEPS, 110, 95
Leung, M., Schwieterman, E. W., Parenteau, M. N., & Fauchez, T. J. 2022, ApJ, 938, 6
Lide, D. 2007, Handbook of Chemistry and Physics 88th Edition ed (CRC Press, Taylor & Francis)
Line, M. R., & Parmentier, V. 2016, ApJ, 820, 78
Liss, P., Malin, G., & Turner, S. 1993, Dimethylsulphide: Oceans, Atmosphere and Climate (Kluwer Dordrecht), 1
Liu, R., Wang, L.-C., Rustamkulov, Z., & Sing, D. K. 2025, AJ, 169, 335
Liu, Y., Shao, M., Fu, L., et al. 2008, AtmEn, 42, 6247
Lueber, A., Novais, A., Fisher, C., & Heng, K. 2024, A&A, 687, A110
Luque, R., Piaulet-Ghorayeb, C., Radica, M., et al. 2025, A&A, 700, A284
MacDonald, R. J. 2023, JOSS, 8, 4873
MacDonald, R. J., & Madhusudhan, N. 2017, MNRAS, 469, 1979
MacLeod, A. J., & Gonzales de Troconis, N. 1982, JAFC, 30, 515
Macleod, A. J., Macleod, G., & Snyder, C. H. 1988, PChem, 27, 2189
Madhusudhan, N., Constantinou, S., Holmberg, M., et al. 2025, ApJL, 983, L40
Madhusudhan, N., Nixon, M. C., Welbanks, L., Piette, A. A. A., & Booth, R. A. 2020, ApJL, 891, L7
Madhusudhan, N., Piette, A. A. A., & Constantinou, S. 2021, ApJ, 918, 1

Madhusudhan, N., Sarkar, S., Constantinou, S., et al. 2023, ApJL, 956, L13
Madhusudhan, N., & Seager, S. 2009, ApJ, 707, 24
Meadows, V., Graham, H., Abrahamsson, V., et al. 2022, arXiv, arXiv:2210.14293
Meadows, V., Orton, G., Liang, M. C., et al. 2006, DPS, 38, 11.35
Mollière, P., Wardenier, J. P., Boekel, R., et al. 2019, A&A, 627, A67
Montet, B. T., Morton, T. D., Foreman-Mackey, D., et al. 2015, ApJ, 809 25
Mungall, E. L., Croft, B., Lizotte, M., et al. 2016, ACP, 16, 6665
Murphy, M. M., Beatty, T. G., Welbanks, L., & Fu, G. 2025, AJ, 169, 286
Nasedkin, E., Mollière, P., & Blain, D. 2024, JOSS, 9, 5875
Niraula, P., De Wit, J., Gordon, I. E., Hargreaves, R. J., & Sousa-Silva, C. 2023, ApJL, 950, L17
Niraula, P., de Wit, J., Gordon, I. E., et al. 2022, NatAs, 6, 1287
Nixon, C. A., Jennings, D. E., Bezard, B., et al. 2013, ApJL, 776, L14
Nixon, M. C., Welbanks, L., McGill, P., & Kempton, E. M.-R. 2024, ApJ, 966, 156
Novais, A., Fisher, C., Ghezzi, L., et al. 2025, MNRAS, 538, 2521
Orton, G. S., Serabyn, E., & Lee, Y. 2000, Icar, 146, 48
Particle Data Group, Workman, R. L., Burkert, V. D., et al. 2022, PTEP, 2022, 083C01
Pilcher, C. B. 2003, AsBio, 3, 471
Pilling, S., Andrade, D. P. P., da Silveira, E. F., et al. 2012, MNRAS, 423, 2209
Pinhas, A., Madhusudhan, N., Gandhi, S., & MacDonald, R. 2019, MNRAS, 482, 1485
Pinhas, A., Rackham, B. V., Madhusudhan, N., & Apai, D. 2018, MNRAS, 480, 5314
Powell, D., Feinstein, A. D., Lee, E. K. H., et al. 2024, Natur, 626, 979
Pozzani, U., Kinkead, E., & King, J. 1968, American Industrial Hygiene Association Journal, 29, 202
Raulin, F., & Toupance, G. 1975, OrLi, 6, 91
Reed, N. W., Shearer, R. L., McGlynn, S. E., et al. 2024, ApJL, 973, L38
Rossabi, S., & Helmig, D. 2018, JGRD, 123, 3772
Sanz-Novo, M., Rivilla, V. M., Endres, C. P., et al. 2025, ApJL, 980, L37
Schauer, J. J., Kleeman, M. J., Cass, G. R., & Simoneit, B. R. 2001, EnST, 35, 1716
Schauer, J. J., Kleeman, M. J., Cass, G. R., & Simoneit, B. R. 2002, EnST, 36, 1169
Schmidt, S. P., MacDonald, R. J., Tsai, S.-M., et al. 2025, AJ, 170, 298
Schwieterman, E. W., Kiang, N. Y., Parenteau, M. N., et al. 2018, AsBio, 18, 663
Schwieterman, E. W., & Leung, M. 2024, RvMG, 90, 465
Seager, S., Bains, W., & Hu, R. 2013, ApJ, 777, 95
Seager, S., Bains, W., & Petkowski, J. J. 2016, AsBio, 16, 465
Seager, S., Welbanks, L., Ellerbroek, L., Bains, W., & Petkowski, J. J. 2025, PNAS, 122, e2416188122
Sellke, T., Bayarri, M. J., & Berger, J. O. 2001, The American Statistician, 55, 62
Serigano, J., Hörst, S. M., He, C., et al. 2022, JGRE, 127, e07238
Simpson, D., Winiwarter, W., BöRjesson, G., et al. 1999, JGR, 104, 8113
Snyder, L. E., & Buhl, D. 1973, NPhS, 243, 45
Sousa-Silva, C., Seager, S., Ranjan, S., et al. 2020, AsBio, 20, 235
Steffens, B. L., Nixon, C. A., Sung, K., et al. 2022, PSJ, 3, 59
Steffl, A. J., Young, L. A., Strobel, D. F., et al. 2020, AJ, 159, 274
Steiner, A. L., Cohen, R. C., Harley, R. A., et al. 2008, ACP, 8, 351
Taylor, F., Atreya, S., Encrenaz, T., et al. 2004, Jupiter. The Planet, Satellites and Magnetosphere, Vol. 1 (Cambridge Univ. Press), 59
Taylor, J. 2025, RNAAS, 9, 118
Thorngren, D. P., Sing, D. K., & Mukherjee, S. 2026, ApJS, 283, 10
Trotta, R. 2008, ConPh, 49, 71
Tsai, S.-M., Innes, H., Wogan, N. F., & Schwieterman, E. W. 2024, ApJL, 966, L24
Tsiaras, A., Waldmann, I. P., Tinetti, G., Tennyson, J., & Yurchenko, S. N. 2019, NatAs, 3, 1086
Turja, A., & Demichela, M. 2011, Chemical Engineering Transactions, 24, 1087
Vastel, C., Ceccarelli, C., Lefloch, B., & Bachiller, R. 2014, ApJL, 795, L2
Visscher, P. T., Baumgartner, L. K., Buckley, D. H., et al. 2003, EnvMi, 5, 296
Waite, J. H., Niemann, H., Yelle, R. V., et al. 2005, Sci, 308, 982
Wang, W., Zhou, R., Jiang, Z.-J., et al. 2014, Advanced Synthesis & Catalysis, 356, 616
Wasserstein, R. L., & Lazar, N. A. 2016, The American Statistician, 70, 129
Welbanks, L., & Madhusudhan, N. 2019, AJ, 157, 206
Welbanks, L., & Madhusudhan, N. 2021, ApJ, 913, 114
Welbanks, L., & Madhusudhan, N. 2022, ApJ, 933, 79
Welbanks, L., McGill, P., Line, M., & Madhusudhan, N. 2023, AJ, 165, 112
Welbanks, L., Nixon, M. C., McGill, P., et al. 2026, NatAs, 10, 234
Yan, S.-B., Li, X.-J., Xu, F., et al. 2023, FrMaS, 10, 1074474
Zhan, Z., Seager, S., Petkowski, J. J., et al. 2021, AsBio, 21, 765